

Lawrence Berkeley National Laboratory

Recent Work

Title

CHARACTERISTICS OF THE HIGH-ENERGY NEGATIVE PHOTOPIONS FROM DEUTERIUM

Permalink

<https://escholarship.org/uc/item/3t414167>

Author

Bandtel, Kenneth C.

Publication Date

1953-07-01

UNIVERSITY OF
CALIFORNIA


*Radiation
Laboratory*

TWO-WEEK LOAN COPY

*This is a Library Circulating Copy
which may be borrowed for two weeks.
For a personal retention copy, call
Tech. Info. Division, Ext. 5545*

BERKELEY, CALIFORNIA

UCRL

2324
cy 

DISCLAIMER

This document was prepared as an account of work sponsored by the United States Government. While this document is believed to contain correct information, neither the United States Government nor any agency thereof, nor the Regents of the University of California, nor any of their employees, makes any warranty, express or implied, or assumes any legal responsibility for the accuracy, completeness, or usefulness of any information, apparatus, product, or process disclosed, or represents that its use would not infringe privately owned rights. Reference herein to any specific commercial product, process, or service by its trade name, trademark, manufacturer, or otherwise, does not necessarily constitute or imply its endorsement, recommendation, or favoring by the United States Government or any agency thereof, or the Regents of the University of California. The views and opinions of authors expressed herein do not necessarily state or reflect those of the United States Government or any agency thereof or the Regents of the University of California.

UCRL-2324
Unclassified - Physics Distribution

UNIVERSITY OF CALIFORNIA
Radiation Laboratory
Contract No. W-7405-eng-48

CHARACTERISTICS OF THE HIGH-ENERGY
NEGATIVE PHOTOPIONS FROM DEUTERIUM

Kenneth C. Bandtel
Thesis
July, 1953

~~AEC COMPUTING FACILITY
INSTITUTE OF MATHEMATICAL SCIENCES
NEW YORK UNIVERSITY
253 GREENE STREET
NEW YORK 3, N. Y.~~

Berkeley, California

CHARACTERISTICS OF THE HIGH-ENERGY
NEGATIVE PHOTOPIONS FROM DEUTERIUM
Table of Contents

Abstract 4

I. Introduction 5

 A. Statement of the Problem and its Significance

 B. Pion-Proton Coincidences Photoproduced
 from Deuterium

 1. Cornell

 2. Berkeley

II. Kinematics and Basic Physics 9

 A. Kinematics of Pion-Proton Coincidences
 Photoproduced from a Free Neutron at Rest

 1. Angular Correlation

 2. Energy Correlation

 B. The Effect of the Exclusion Principle in the Photo-
 production of Pions from Deuterium

 1. General Discussion

 2. Previous Experimental Work

III. Le Levier's Theoretically Predicted Pion Spectra 15

 A. Qualitative Description of the Calculation

 B. The Calculated Spectra

IV. The Experimental Method 18

 A. Basic Description of the Method

 B. The Targets

 C. The Scintillation Counter Telescopes

 D. The Electronic Instrumentation

 1. The Photomultiplier Circuit

 2. The Pulse-Shaping Circuit

 3. The Crystal Diode Coincidence Circuit

 4. The Pulse-Lengthening Amplifier

V. Three-Body Kinematics of the Reaction $\gamma + d \rightarrow \pi^- + p + p$
 27

 A. The Correlation between Pion and Proton Energies
 for a Given Photon Energy

 B. Kinematics of the Reaction Expressed in Terms
 of the Experimentally Measured Quantities

 C. Resolution Function of the Coincidence System

 D. The Experimental Separation of the Condition of
 Low Relative Energy for the Two Final Nucleons

 E. The Measurements That Were Taken

VI.	Folding the Theoretically Predicted Spectra into the Experimental Resolution of the Equipment.	36
	A. General Discussion	
	B. Pion Time of Flight	
	C. Proton Time of Flight	
	D. The Photon Source	
	E. Pion Corrections	
	F. Multiple Scattering of the Proton	
	G. Calculation Procedure	
VII.	Results and Conclusions.	47
	A. Experimental Results	
	B. Relative Counting Rates Predicted from Theory	
	C. An Approximate Correction for the Nonrelativistic Approximation for the Nucleon Energies Used in the Theory	
	D. Discussion of Results and Conclusions	
	Acknowledgments.	54
	Appendices	
	A. Appendix I.	55
	B. Appendix II.	59
	References	61

CHARACTERISTICS OF THE HIGH-ENERGY
NEGATIVE PHOTOPIONS FROM DEUTERIUM

Kenneth C. Bandtel
Thesis

Radiation Laboratory, Department of Physics
University of California, Berkeley, California

July, 1953

ABSTRACT

Negative pions photoproduced from deuterium by the 330-Mev bremsstrahlung of the Berkeley synchrotron have been investigated by observing pion-proton coincidences. A $(CD_2)_n - (CH_2)_n$ subtraction yields the neutron contribution. The purpose of the investigation is to determine how often the initial triplet spin state of the deuteron changes to a singlet spin state for the two final identical nucleons, in the reaction $\gamma + d \rightarrow \pi^- + p + p$. Dr. R. E. Le Levier has calculated the energy spectrum produced assuming 1) the spin state always remains the same, and 2) the spin state always changes. The experimental measurements are integral over meson energy from a lower limit upwards, and also over the time of flight between the proton and the pion. Thus, when Le Levier's spectra are folded into the experimental resolution of the equipment and the bremsstrahlung spectrum they yield a number proportional to the experimental measurement. The ratios of various experimental measurements are compared with the theoretically predicted ratios. Within the limitations of the theory (which uses a nonrelativistic expression for the nucleon energies) and the accuracy of the experimental measurements, the results indicate an interaction intermediate between the two extremes.

CHARACTERISTICS OF THE HIGH-ENERGY NEGATIVE PHOTOPIONS FROM DEUTERIUM

Kenneth C. Bandtel

Radiation Laboratory, Department of Physics
University of California, Berkeley, California

July, 1953

I. INTRODUCTION

A. Statement of the Problem and its Significance

After charged pions produced by photons were discovered (Reference 16 contains a summary of the early photopion production experiments), one of the first things to be measured was the ratio of the photoproduction of negative pions to that of positive pions. The simplest nucleus which can produce both negative and positive pions is deuterium (it is believed impossible to produce negative pions from a proton or positive pions from a neutron). Thus, the minus-plus ratio of pions photoproduced from deuterium should give a comparison of the $\gamma - p$ and the $\gamma - n$ interaction.

White¹⁶ has measured the minus-plus ratio from deuterium at angles of 45° , 90° , and 135° , and at several energies for each angle. He finds that the ratio is close to one, within statistics, in all cases measured. The results of Littauer and Walker¹⁸ and of Lebow et al¹⁷ are in agreement with White's. The unity ratio suggests that the production of positive and negative pions is symmetrical except for the sign of the charge.

Theoretical calculations of the minus-plus ratio have been made, and they are listed in References 36 and 18 of White's paper. When the electromagnetic interaction of the photons with the currents due to moving charges is considered, then the minus-plus ratio is strongly dependent on pion energy and angle of production. However, when the interaction of the photon with the static magnetic moments of the nucleons is considered, then a minus-plus ratio close to unity is predicted which is nearly independent of the angle or energy of the pion. This latter agreement suggests that the interaction between photons and nucleons that results in production of pions may depend on the spin of the nucleon.

In view of this, it is reasonable to ask what fraction of the time the spin of the nucleon "flips over" in the act of photoproduction, if at all. In other words, how often does the deuteron triplet spin state go over into a singlet spin state for the two final nucleons, after photo-pion production.

Since we are left with two identical nucleons after charged photo-pion production, the Pauli exclusion principle is operative and thus half of the quantum states are excluded. This effect is quite pronounced if it is possible to select primarily those dynamical configurations of the reaction $\gamma + d \rightarrow \text{charged pion} + 2 \text{ nucleons}$ that correspond to a low relative energy (and hence an S-state for the two final nucleons). The purpose of the present investigation is to attempt to determine what fraction of the time "spin flip" occurs in the production of negative pions from deuterium.

B. Pion-Proton Coincidences Photoproduced from Deuterium

1. Cornell

Keck and Littauer^{1, 2} have studied the reaction $\gamma + d \rightarrow \pi^- + p + p$ at Cornell by bombarding targets of D_2O and H_2O with bremsstrahlung from the Cornell 310-Mev electron synchrotron. The pion and one of the protons were detected in coincidence. Pions emitted at $90^\circ \pm 10^\circ$ with an energy of 56 ± 9 Mev were identified by their specific ionization and range. The protons were detected by a 6.55 g/cm^2 NaI(Tl) crystal and their energy was measured using a pulse-height analyzer. Keck and Littauer measured the cross section as a function of the proton energy, at a proton angle of $30^\circ \pm 6^\circ$. They also varied the proton angle and measured the cross section integrated over proton energy. The expected angle and energy distribution were computed for the following cases:

- (1) Assuming production from a free neutron at rest, and taking account of the geometry of the experiment.
- (2) Taking into account the internal momentum of the deuteron, assuming the zero range wave function and no momentum transfer to the "spectator" proton.

The latter calculation gave satisfactory agreement with experiment, which supports the assumption of negligible momentum transfer to the "Spectator" proton. The cross section obtained was $10.8 \pm 1.0 \mu\text{b/sterad.}$ for production at 90° in the laboratory by 236-Mev photons. The cross section for production of negative pions without the requirement of a correlated recoil was also determined, using the π^-/π^+ ratio of Littauer and Walker³ to separate the π^- and π^+ contributions in the telescope. The value $11.8 \pm 1.2 \mu\text{b/sterad.}$ was obtained. They state that the agreement between the two cross sections may be taken as evidence that the "spectator process" does account for a substantial fraction of the meson production in the deuteron at the angles and energies involved.

This⁴ at Cornell has applied the theory developed by Chew and Lewis⁹ to explain the experimental energy distribution of recoils measured by Keck and Littauer. The general shape of the curve he obtains corresponds with the experimentally measured points; however, This states that both the half-width and the location of the maximum are at variance with experiment.

2. Berkeley

Madey, Frank and Bandtel^{5,6} have studied the reaction $\gamma + d \rightarrow \pi^- + p + p$ at Berkeley using the 320-Mev bremsstrahlung of the Berkeley synchrotron, and a $\text{D}_2\text{O} - \text{H}_2\text{O}$ difference. Pion-proton coincidences were observed at those angles predicted by the conservation laws for the photoproduction of a pion from a free neutron at rest. The predicted pairs of correlated pion and proton angles remain very nearly the same for photon energies of 220 to 320 Mev. Thresholds for the detection of protons and pions were set by using absorbers in the proton and pion telescopes. Thus, the minimum photon energy that could contribute was determined by these absorbers. The proton angle was varied, keeping the pion angle fixed. It was found that the counting rate exhibited a well defined peak at the pair of angles predicted for production from a free neutron at rest. Enough absorber was added, first in one telescope and then in the other, to stop the maximum expected energy pion or proton photoproduced from a free neutron at

rest by the maximum energy photon available. This reduced the counting rate to zero, within statistics. This evidence shows that the supposed particles have the correct range. Also, the counting rate greatly decreased when the pion telescope was tilted out of the plane. This provides evidence that the process is essentially coplanar.

Both the work at Cornell and that at Berkeley provide evidence that a large fraction of the π^- production arises from the neutron in a loosely-bound state, and that the angle and energy correlations of production from the neutron are those of production from a free neutron at rest which has been smeared out by the internal momentum of the deuteron.

II. KINEMATICS AND BASIC PHYSICS

A. Kinematics of Pion-Proton Coincidences Photoproduced from a Free Neutron at Rest

The kinematics of the reaction $\gamma + n \rightarrow \pi^- + p$, where the neutron is assumed to be at rest and free, will be reviewed briefly for comparison with the three-body kinematics discussed later.

1. Angular Correlation

The angular correlation is shown in Fig. 1. Proton angle is plotted versus pion angle for various photon energies from near threshold to 1000 Mev. Note that the correlation angles are nearly independent of photon energy for the range of photon energies from 230 to 330 Mev.

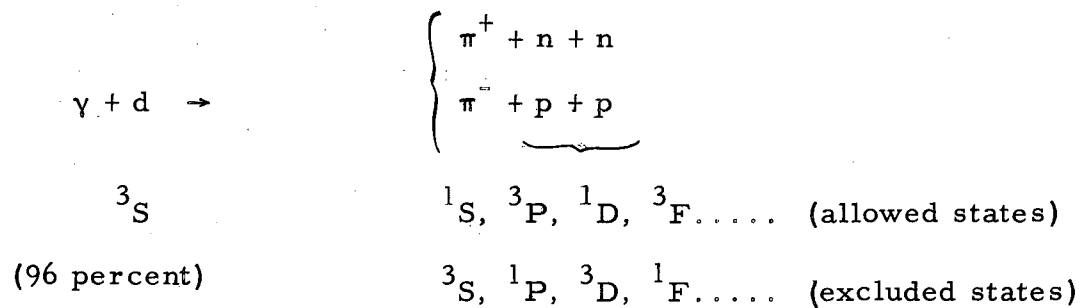
2. Energy Correlation

The energy correlation is shown in Fig. 2. Lines of constant proton angle and lines of constant photon energy are plotted on the plane of proton kinetic energy versus pion kinetic energy. This can be contrasted with Fig. 1. There is an angular correlation over a range of photon energies that is much closer than the correlation of proton or pion energies.

B. The Effect of the Exclusion Principle in the Photoproduction of Pions from Deuterium

1. General Discussion

Consider the reactions



The deuteron is initially in the 3S state (96 percent). After photoproduction the two remaining nucleons are identical. Since two identical nucleons obey the Pauli Exclusion Principle they can only be in anti-symmetric

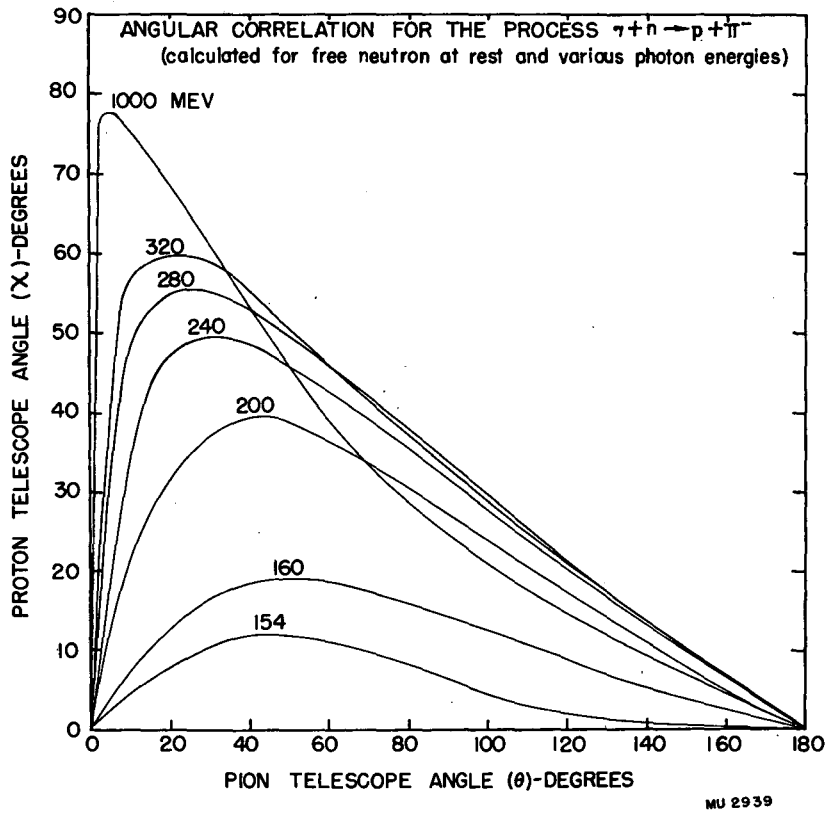


Fig. 1.
The Angular Correlation
of the Process $\gamma + n \rightarrow \pi^- + p$

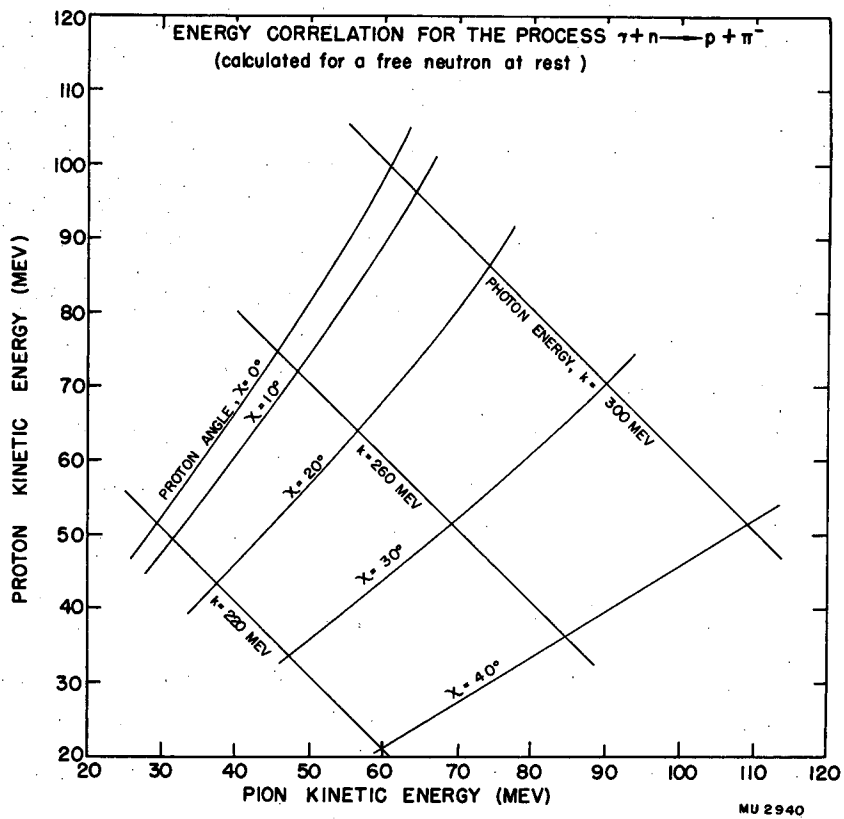


Fig. 2.
 The Energy Correlation
 of the Process $\gamma + n \rightarrow \pi^- + p$

states. Therefore, unless the spin of the neutron "flips" over in the act of photoproduction, S states for the two final nucleons will be excluded, the available phase space will be reduced, and thus the cross section for photoproduction from a bound nucleon in deuterium will be reduced relative to production from a free nucleon.

This exclusion of S states for the two final nucleons obviously has the most pronounced effect under conditions wherein the two final nucleons are in an S state the majority of the time. This occurs when these two final nucleons are left with low relative energy after meson production. Three-body kinematics for the reaction $\gamma + d \rightarrow \text{charged pion} + 2 \text{ nucleons}$ lead to the result that this condition of low relative energy for the two final nucleons occur (1) at threshold, (2) when the mesons are emitted in the forward direction in the laboratory, and (3) near the upper end of the meson spectrum, for a given photon energy.

Feshbach and Lax^{7, 8, 10}, Chew and Lewis⁹, Machida and Tamura¹², Saito, Watanabe and Yamaguchi¹¹, and LeLevier¹³, have made the theoretical investigations of the photoproduction of pions from deuterium, using the impulse approximation and a phenomenological treatment which does not depend on a detailed meson theory. Morpurgo¹⁴ has also investigated this problem theoretically.

Chew and Lewis⁹ point out that an experimental comparison of the deuteron and proton cross sections for the production of positive pions near zero degrees to the beam can be used to determine the nucleon spin-flip probability in the reaction $\gamma + d \rightarrow \pi^+ + n + n$. They calculate the distribution of nucleon recoils and the pion angular distribution, employing "closure theorems" in an approximation such that the final state of the two nucleons can remain unspecified. This approximation tends to overestimate the production from deuterium slightly, since it includes some final states that are not energetically possible.

Feshbach and Lax¹⁰ have calculated the pion spectrum at a given angle to the incident photon beam. For high photon energies they employed the "closure approximation". At low and intermediate photon energies the closure approximation was not made, but the neutron-neutron force

in the final nucleon state was neglected. They integrated their pion spectra over a bremsstrahlung spectrum of photon energies. They also found the total cross section at high photon energies and near the threshold for meson production. The calculations of Chew and Lewis and of Feshbach and Lax are very similar. According to Feshbach and Lax, the principal difference is that Chew and Lewis focus their attention on the distribution of nuclear recoils, whereas Feshbach and Lax are interested primarily in the energy spectrum of pions at a given production angle.

Saito, Watanabe and Yamaguchi¹¹ computed the energy spectra at three angles (0° , 45° , 90°) for incident γ -ray energies of 200, 250, 300, and 350 Mev.

Machida and Tamura¹² calculated the energy spectra at 0° and 90° produced by 340-Mev monochromatic γ -rays, and also the spectrum produced at 90° by a 340-Mev bremsstrahlung spectrum. It appears that their calculations are only applicable when the two final nucleons are in a 1S state.

Le Levier¹³ calculated the pion spectra for various photon energies, under the condition of fixed recoil angles for the pion and one of the protons. This calculation forms the basis of the present experiment and is discussed in detail in a later section.

2. Previous Experimental Work

Any of these theories predict a large exclusion effect for photoproduced pions from deuterium, when the pions are emitted near zero degrees to the beam. Therefore, a straightforward way to determine experimentally the effect of the exclusion principle would be to observe pions emitted at zero degrees.

Unfortunately this is difficult to do experimentally. Jarmie¹⁵ set out to measure the ratio of the cross sections for the production of positive pions from deuterium and hydrogen at zero degrees. He originally attempted to use electronic equipment to detect the π - μ decay of the positive pion. However, the large background of electrons and positrons in the forward direction made this very difficult. Subsequently, he used photographic plate techniques successfully. Unfortunately, the cross

section for π^+ production at zero degrees happens to be lower than at other angles. In fact, Jarmie scanned 9.03 cm^2 of emulsion and found ten events. He quotes a cross section of $\boxed{6.2 - 1.9}^{+2.6} \times 10^{-30} \text{ cm}^2 \text{ ster.}^{-1}$ proton⁻¹ quanta⁻¹ for the cross section of $\gamma + p \rightarrow \pi^+ + n$ at a photon energy of $278 \pm .4 \text{ Mev}$ and at 0 ± 4 degrees to the beam direction. This corresponds to a meson energy of $134 \pm 4 \text{ Mev}$.

Jarmie then bombarded deuterium. He scanned 8.97 cm^2 of emulsion and found four events. The ratio of production from deuterium to production from hydrogen was about 0.4. He does not draw any conclusions about the spin-flip probability.

White¹⁶ has measured the cross section for production of charged photopions from deuterium and hydrogen at 45° , 90° , and 135° . The exclusion effect here is not so large as at zero degrees, and this makes it more difficult to measure the effect of the exclusion principle. White does not draw any conclusions about the spin-flip probability. However, he compares his data with the theory of Chew and Lewis, and concludes that the data give strong support to the validity of the impulse approximation.

Lebow, Feld, Frisch and Osborne¹⁷ have measured the energy distributions of charged photopions from hydrogen and deuterium at 90° and 26° to the photon beam. They compare the ratio of positive pions from deuterium and hydrogen with a phenomenological meson theory of Feshbach and Lax for different laboratory pion angles in Fig. 2 of their article. The data of White¹⁶ (at laboratory angles of 45° , 90° and 135°) and Littauer and Walker¹⁸ (at a laboratory angle of 135°) are also plotted. Lebow et.al state that the data suggest that there is a large spin-dependent interaction. The data at 90° (of both White and Lebow et al) would tend to suggest no spin-dependent interaction; however, the difference produced by these two degrees of spin interaction is more pronounced at forward laboratory angles than for backward angles, and the 26° point favors a large spin-dependent interaction.

III. LE LEVIER'S THEORETICALLY PREDICTED PION SPECTRA

A. Qualitative Description of the Calculation

LeLevier¹³ has calculated the spectrum of negative pions produced by monoenergetic photons on deuterium for the pion at 120° and one of the protons at 20° . These recoil angles result when a pion is photo-produced from a free neutron at rest, for an incident photon energy of about 280 Mev. (Figure 1 shows that these correlated recoil angles remain very nearly the same for photon energies from 240 to 320 Mev.) The calculation uses the impulse approximation¹⁹ and a phenomenological spin-dependent interaction.⁸ The emitted meson is treated relativistically and the two final nucleons are treated nonrelativistically. The calculation has been carried out using a Hulthen wave function for the initial deuteron,

$$\psi = N \frac{e^{-\alpha r} - e^{-\beta r}}{r},$$

with $\beta / \alpha = 7$.

The excitation function for the process $\gamma + d \rightarrow \pi^- + p + p$ has been assumed constant as a function of incident photon energy, since the excitation function for the production of positive pions by photons on hydrogen is essentially flat²⁰ for photon energies from 260 Mev to 310 Mev. If the excitation function for negative pions is the same as that for positive pions in this photon energy region, then this is a satisfactory approximation.

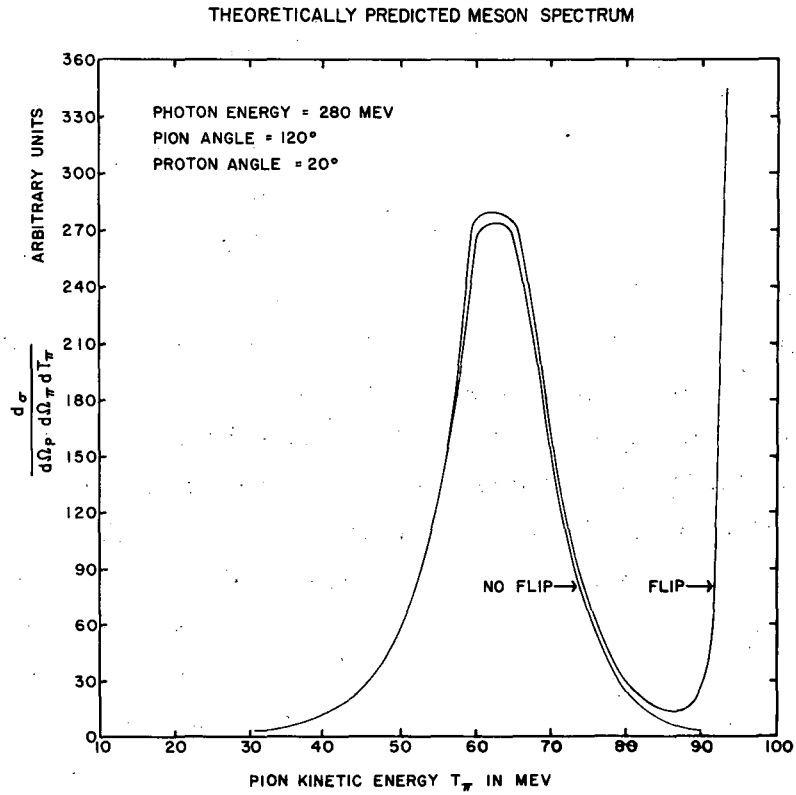
The wave functions of the two final nucleons have been taken to be plane waves in all but the S-state of relative angular momentum. In the 1S state, the 1S interaction, corrected for coulomb scattering, has been obtained by fitting data from low-energy p - p scattering experiments.

As has been mentioned, the only available states for the two final identical nucleons are odd states, 1S , 3P , 1D , 3F . Le Levier calculated these spectra under two assumptions: (1) Assuming that the spin state of the two final nucleons is a triplet state; these spectra are designated "no flip", which refers to the fact that the spin of the neutron does not

flip over in the act of photoproduction. This would leave available the 3P , 3F ... et cetera, states. (2) Assuming that the final spin state of the nucleons is a singlet state; this would leave available the 1S , 1D ... et cetera, states. Since the upper part of the pion spectra produced by a monoenergetic photon is kinematically associated with an S state for the two final nucleons, this second assumption gives a larger ordinate for the upper end of the pion spectra than assumption (1). These spectra are designated "flip".

B. The Calculated Spectra

A typical theoretically predicted pion spectrum of Le Levier is shown in Fig. 3. This particular spectrum is calculated for 280-Mev photons incident. The broad maximum has its peak at the unique energy which would be expected for production from a free neutron at rest. This part of the spectrum will be designated as the "free production peak". The sharp rise at maximum meson energy in the case of a final singlet spin state will be called the "spin-flip spike". For a given photon energy, momentum and energy conservation laws for this three-body reaction show that the pion energy is a maximum when the two protons have low relative energy. At the maximum pion energy possible for this photon energy, and with the pion angle as specified, both protons have about 20 Mev in the laboratory even though their relative energy is less than 1 Mev. (See Fig. 10.) Such low relative energy protons would be in 1S -state. Spectra have been calculated for incident photon energies from 240 to 320 Mev.



MU-5281

Fig. 3.
The Theoretically Predicted
Pion Spectra $\gamma + d \rightarrow \pi^- + p + p$

IV. THE EXPERIMENTAL METHOD

A. Basic Description of the Method

Figure 4 illustrates the physical arrangement of the present experiment. The location of the pion and proton telescopes and the target are shown with respect to the beam direction. The pion and proton telescopes are coplanar.

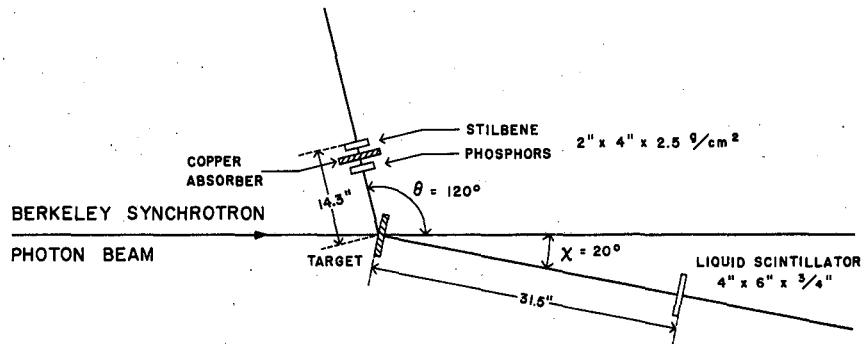
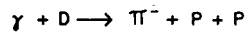
The basic method of the experiment is the observation of negative pion-proton coincidences. A $\text{CD}_2 - \text{CH}_2$ difference is used for the target. This insures that we have a negative pion-proton coincidence, provided both coincident particles are charged.

The only other reaction which could contribute would then be $\gamma + d \rightarrow \pi^0 + d$. This contribution is thought to be small for the following reasons: (1) The π^0 mesons which start out in a given direction are smeared over a range of angles when they decay into photons. (2) Only four percent of the γ -rays incident upon the first scintillator are converted by it. (3) Of those that are converted, only resultant electrons with energy greater than 26 or 48 Mev (depending on the absorber) penetrate the absorber between the π -1 and π -2 scintillators. (4) This reaction has a different angular correlation than the angles at which the present experiment was conducted. For $\gamma + d \rightarrow \pi^0 + d$, $120^\circ \pm 3.5^\circ$ is correlated with $26.2^\circ \pm 1.6^\circ$. The observations of the present experiment were made at $120^\circ \pm 3.5^\circ$ and $20^\circ \pm 3.6^\circ$.

Figure 5 is a block diagram of the electronics.

Besides the correlated angles, the two things that are experimentally determined are (a) the minimum pion energy, and (b) the time-of-flight difference between the proton and the negative pion. The minimum pion energy is determined by putting copper absorber between the π_1 and π_2 counters. The time of flight difference between the proton and pion is determined within the limits of the resolution function of the equipment. This is explained more completely in a later section.

EXPERIMENTAL ARRANGEMENT



MU-5282

Fig. 4.
The Physical Arrangement
of the Experiment

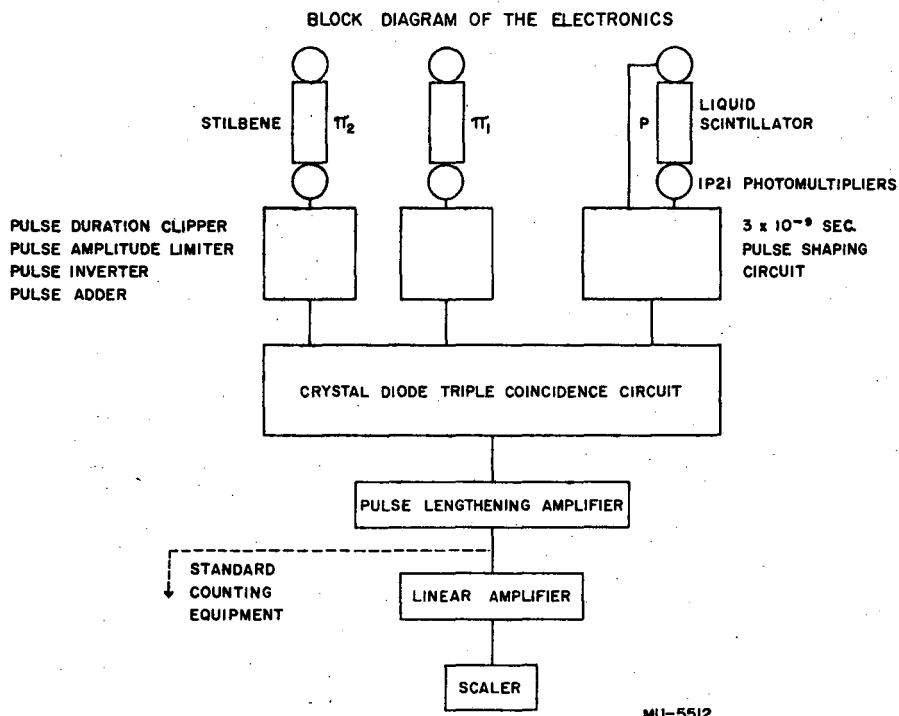


Fig. 5
Block Diagram of the Electronic
Instrumentation

B. The Targets

A CD_2 target 131 milligram/ cm^2 thick and 1.75 inches in diameter was used. This target was loaned to the author by Dr. David Clark. The CH_2 target that was used for the subtraction was 115 milligrams/ cm^2 thick and about the same diameter.

The CD_2 target was pressure molded with enough heat applied to the mold to melt the CD_2 . The CH_2 target was cut from a sheet of polyethylene which was checked for uniform density. Both targets were suspended by threads at three points around the periphery. These threads were fastened to a larger concentric three-inch-diameter brass support ring.

The CH_2 and CD_2 targets contain the same number of molecules per square centimeter to less than five percent accuracy. The synchrotron beam did not overlap the edges of the target.

C. The Scintillation Counter Telescopes

The proton telescope consisted of a four-inch by six-inch liquid scintillation counter, three-fourths inch thick, viewed at each of the four-inch ends by 1P21 photomultiplier tubes.

The pion telescope consisted of two 1-3/4 inch by four-inch by 2.5 g/ cm^2 stilbene crystals. These were viewed at each end by 1P21 photomultiplier tubes.

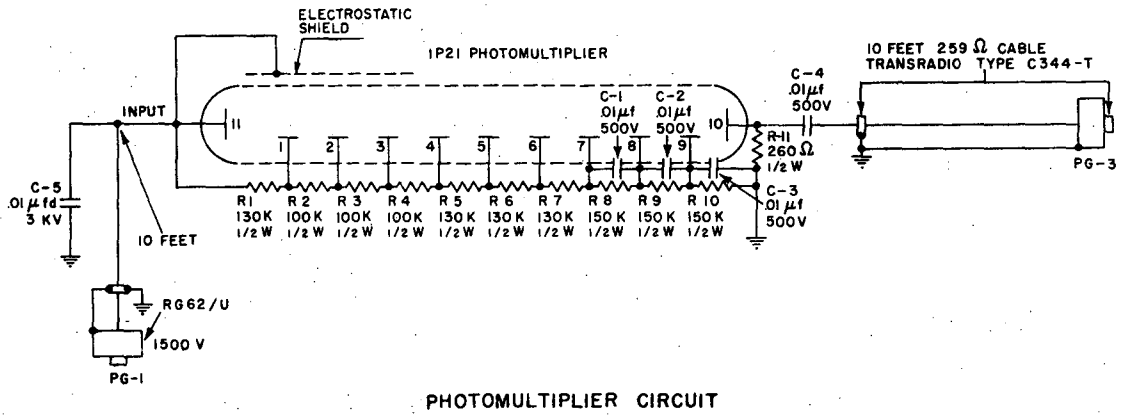
D. The Electronic Instrumentation

1. The Photomultiplier Circuit

The electronic instrumentation is described in detail in an article to be published by Dr. R. Madey, hence the electronics are described only briefly here. The photomultiplier circuit is shown in Fig. 6. The output of the photomultiplier circuit is connected to the input of the pulse-shaping circuit by means of Transradio Type C344-T 259 Ω cable.

2. The Pulse-Shaping Circuit

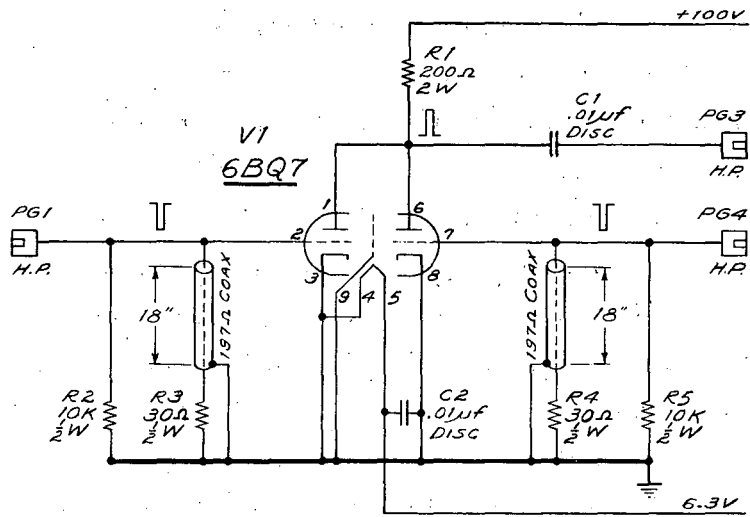
The pulse-shaping circuit is shown in Fig. 7. The outputs of the two 1P21 photomultiplier tubes that view a common scintillator, are connected to the two inputs of a single pulse-shaping circuit. These two pulses are combined in the pulse-shaping circuit. The pulse-shaping



PHOTOMULTIPLIER CIRCUIT

MU-5887

Fig. 6
Photomultiplier Circuit



MILLIMICROSECOND PULSE LIMITER
& ADDER

MU-5253

Fig. 7
The Pulse Shaping Circuit

circuit also performs the functions of limiting the pulses in amplitude to several volts, and limiting the pulse in time by means of a piece of nearly shorted transmission cable connected in the grid circuit. The length of this "clipper" is 18 inches, which corresponds to a nominal pulse length of about 3.2×10^{-9} sec.

3. The Crystal Diode Coincidence Circuit

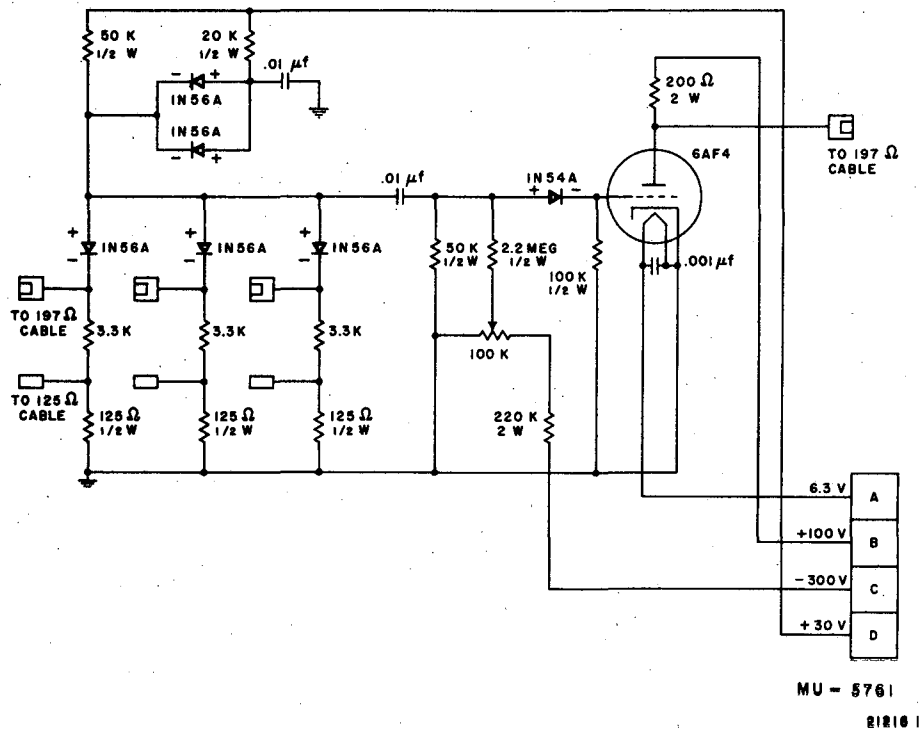
The crystal diode triple coincidence circuit is shown in Fig. 8. The output of the pulse-shaping circuit is connected to the input of the coincidence circuit by Transradio Type C3-T 197 Ω cable. Any time-of-flight delay between the various pulses is inserted at this point. Once the coincidence has been made with time resolution of about 3×10^{-9} seconds, it is necessary to lengthen the output pulse to about 10^{-6} second in order to be able to count it with standard counting equipment. The output section of the coincidence circuit is designed to lengthen the coincidence pulse somewhat.

4. The Pulse-Lengthening Amplifier

The pulse-lengthening amplifier used is the first model of the one shown in Fig. 9. It differs from the one shown in the following respects: The resistor R-24 was not present, and the IN56A diode that connects to the top of R-24 was replaced by a piece of wire.

This amplifier lengthens and amplifies the coincidence pulses so they will be suitable for use in standard microsecond counting equipment.

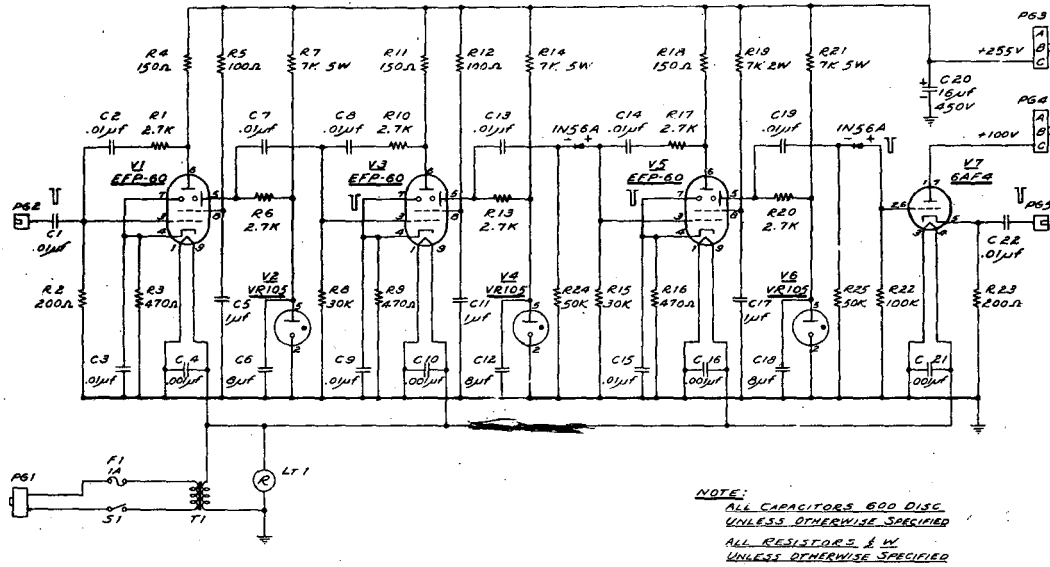
CRYSTAL DIODE TRIPLE COINCIDENCE CIRCUIT



MU - 5761

212161

Fig. 8.
The Crystal Diode Triple
Coincidence Circuit.



REV	DESCRIPTION	DATE	BY	CHKD	APPROVED
1	SCHEMATIC				
2	...				
3	...				
4	...				
5	...				
6	...				
7	...				
8	...				
9	...				
10	...				

Fig. 9
The Pulse Lengthening
Amplifier

V. THREE-BODY KINEMATICS OF THE REACTION $\gamma + d \rightarrow \pi^- + p + p$

A. The Correlation between Pion and Proton Energies for a Given Photon Energy

Let us apply energy- and momentum-conservation equations to the reaction $\gamma + d \rightarrow \pi^- + p + p$ and impose the conditions that the negative pion and one of the protons be coplanar and at fixed angles in this plane. * Conservation of momentum normal to this plane shows that the other proton will also be in this plane. This leaves two momentum-conservation equations in this plane and one energy-conservation equation, i. e., three equations. On the other hand, we have five unknowns: the γ -ray energy, the pion energy, the energy of the first proton, the energy of the second proton, and the angle of the second proton.

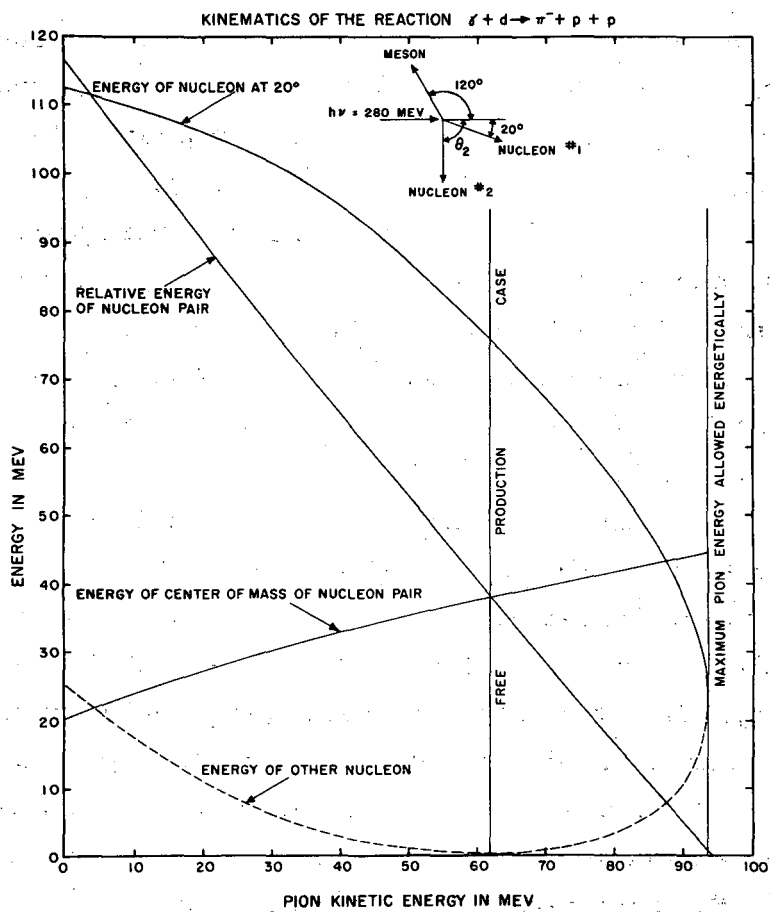
Thus, if we consider the spectrum produced by a particular γ -ray energy, and consider a particular pion energy on this spectrum, then these two additional parameters completely specify the dynamical state of the reaction. This means that each pion energy in Fig. 3 (which is calculated for a given photon energy) is associated with a unique proton energy at 20° .

For a given photon energy of 280 Mev, Fig. 10 shows the energy correlations. The final relative energy of the nucleon pair, the energy of the center of mass of the two nucleons, the energy of the nucleon at 20° , and the energy of the other nucleon are plotted as a function of the pion energy. Note that when the maximum possible pion energy is approached, both nucleons tend to about 22 Mev and the relative energy of the two final nucleons decreases. As was mentioned before, this is the region where the exclusion principle has an appreciable effect on photomeson production.

B. Kinematics of the Reaction Expressed in Terms of the Experimentally Measured Quantities

The minimum pion energy and the time-of-flight difference between the proton and the pion are the quantities that are experimentally measured.

* See Appendix I



MU- 5779

Fig. 10.
 Energy Correlation of
 the Reaction $\gamma + d \rightarrow \pi^- + p + p$
 for a Photon Energy of 280 Mev.
 Various Energies are shown as
 a function of the pion kinetic
 energy.

The minimum pion energy is determined by the amount of absorber placed between the first and second pion counters. Any pion with more energy than this minimum amount can contribute to a coincidence; hence the pion energy measurement is integral from some minimum value up to the maximum energy available.

The other quantity which is experimentally measured is the time-of-flight difference between the proton and the pion. This time-of-flight difference is measured within the width of the resolution function of the coincidence system. By "resolution function" we mean a function that gives the detection efficiency as a function of the difference in delay between the input pulses to the coincidence circuit. Thus, the time-of-flight measurement is integral over the time width of the resolution function of the equipment, with a relative weight given by the form of that function for a particular difference in delay.

The time-of-flight difference between the proton and pion can be calculated if we know the energies involved. This is explained later in more detail. For the present experiment the proton is moving more slowly than the pion, in general, and the proton counter is further away from the target than the pion counter. This means that the proton pulse occurs later in time than the pion pulse. Hence, in order to record a pion-proton coincidence which has a time-of-flight difference τ_0 with full efficiency, a length of cable that provides a time delay of τ_0 must be inserted between the pion counter and the input to the coincidence circuit. If the coincidence system had an infinitely sharp resolution function, and a fixed delay τ_0 were inserted in the input to the coincidence circuit, then only those events with a time-of-flight difference exactly equal to τ_0 would be recorded. In actuality the coincidence system resolution $r(\tau)$ measures the probability that a coincidence will be recorded, if there is a delay τ between the input pulses to the coincidence circuit. Thus, if a time-of-flight delay τ_0 is inserted in one input to the coincidence circuit, and if τ is the time-of-flight delay for the coincident process we are considering, then the probability of observing coincidences will be proportional to $r(\tau - \tau_0)$. The next section describes how the resolution function was measured.

C. Resolution Function of the Coincidence System

The resolution function of the coincidence system $r(\tau')$, was measured in the following way: simultaneous pulses were fed into the coincidence circuit, with no delay between the inputs, at a fixed rate of N_0 pulses per minute. Since this coincidence system has been determined (from other measurements) to be almost 100 percent efficient with no delay between the inputs, we know it will record coincidences at a rate essentially equal to N_0 . This counting rate gives a number proportional to $r(\tau'=0)$. Then a length of cable is added in one input to the coincidence circuit corresponding to a net delay $\tau'=\tau_1$. The coincidence counting rate under this second condition gives a number proportional to $r(\tau'=\tau_1)$. Proceeding in this fashion, by adding delays and measuring counting rates one obtains counting rates as a function of net delay, τ' . Thus, one obtains the detection efficiency as a function of the net delay between the input pulses to the coincidence circuit.

D. The Experimental Separation of the Condition of Low Relative Energy for the Two Final Nucleons

Le Levier's calculated spectra show that the free-production peak and the spin-flip spike are the two most dominant parts of the spectra, since the heaviest weight is associated with these two regions. Table I shows the pion and proton energies associated with the free-production peak and spin-flip spike for photon energies from 260 to 320 Mev.

For this range of photon energies, the pion energies in the spin-flip spikes are greater than the pion energies in the free-production peaks. These two ranges of pion energies are separable by means of absorbers. We will see that the protons correlated with the peaks and the tails fall into two groups, which are separable by time of flight. In fact, time of flight alone produces a fairly clean separation of the condition of low relative energy from the quasi free-production condition.

Figure 11 illustrates the kinematical features of the reaction $\gamma + d \rightarrow \pi^- + p + p$ for the particular geometry under which this experiment was conducted. The time-of-flight difference between proton and pion is plotted against pion energy. If production were from a free neutron at rest, $\gamma + n \rightarrow \pi^- + p$, then there would be only one point on Fig. 11 for a

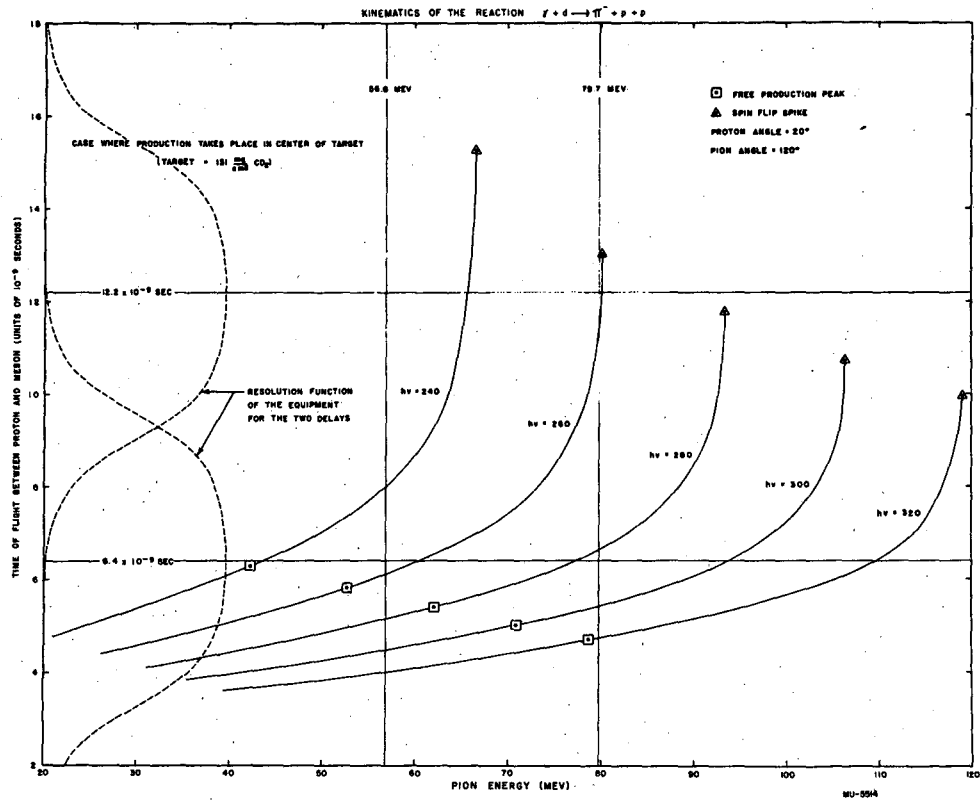


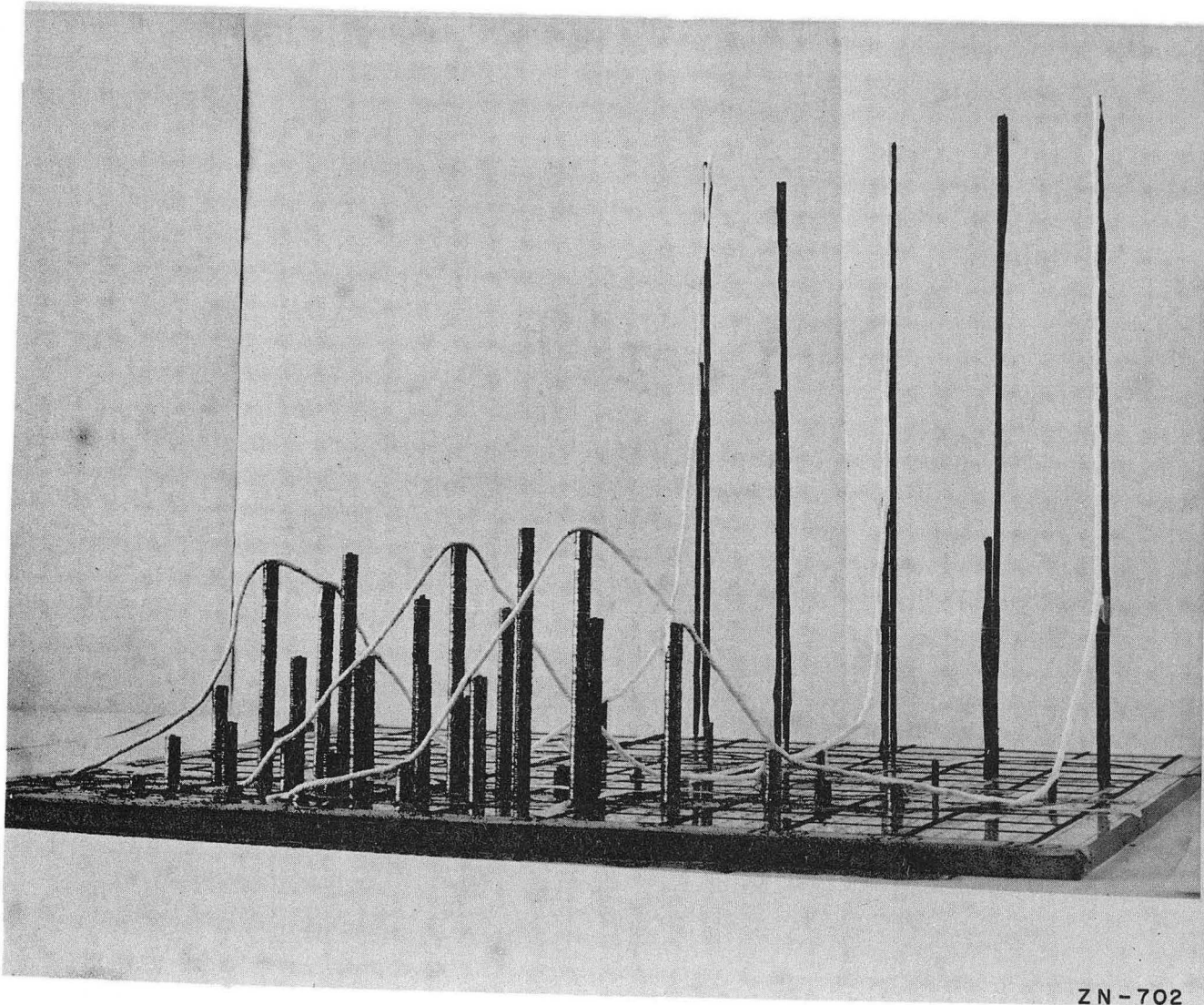
Fig. 11.
Kinematics of the Reaction
 $\gamma + d \rightarrow \pi^- + p + p$ for the
Particular Geometry of the
Present Experiment. The
time of flight difference
between the Proton and Pion
is plotted against pion energy.

given photon energy. This point is enclosed by a square. Since production is taking place from a neutron which has a momentum distribution, the dynamical configurations possible for a given photon energy now take the form of a line. This line corresponds to the spectrum for a constant photon energy, which was plotted in Fig. 3. The spin-flip spike is indicated by the point enclosed by a triangle. Figure 11 merely indicates the dynamical configurations possible. The probability of occurrence of a particular dynamical configuration, that is the ordinate of the spectrum that Le Levier calculated, might be thought of as plotted in a third dimension normal to the plane of the paper. In other words a certain "weight" is associated with each point of Fig. 11.

Figure 12 shows various photographs of a three-dimensional model designed to illustrate this feature pictorially. The ordinates of the theoretically predicted spectra are plotted normal to the plane of Fig. 11. The broad ridge corresponds to the free-production peaks for the various photon energies, and the spin-flip spikes form the sharp ridge on the other side of the valley.

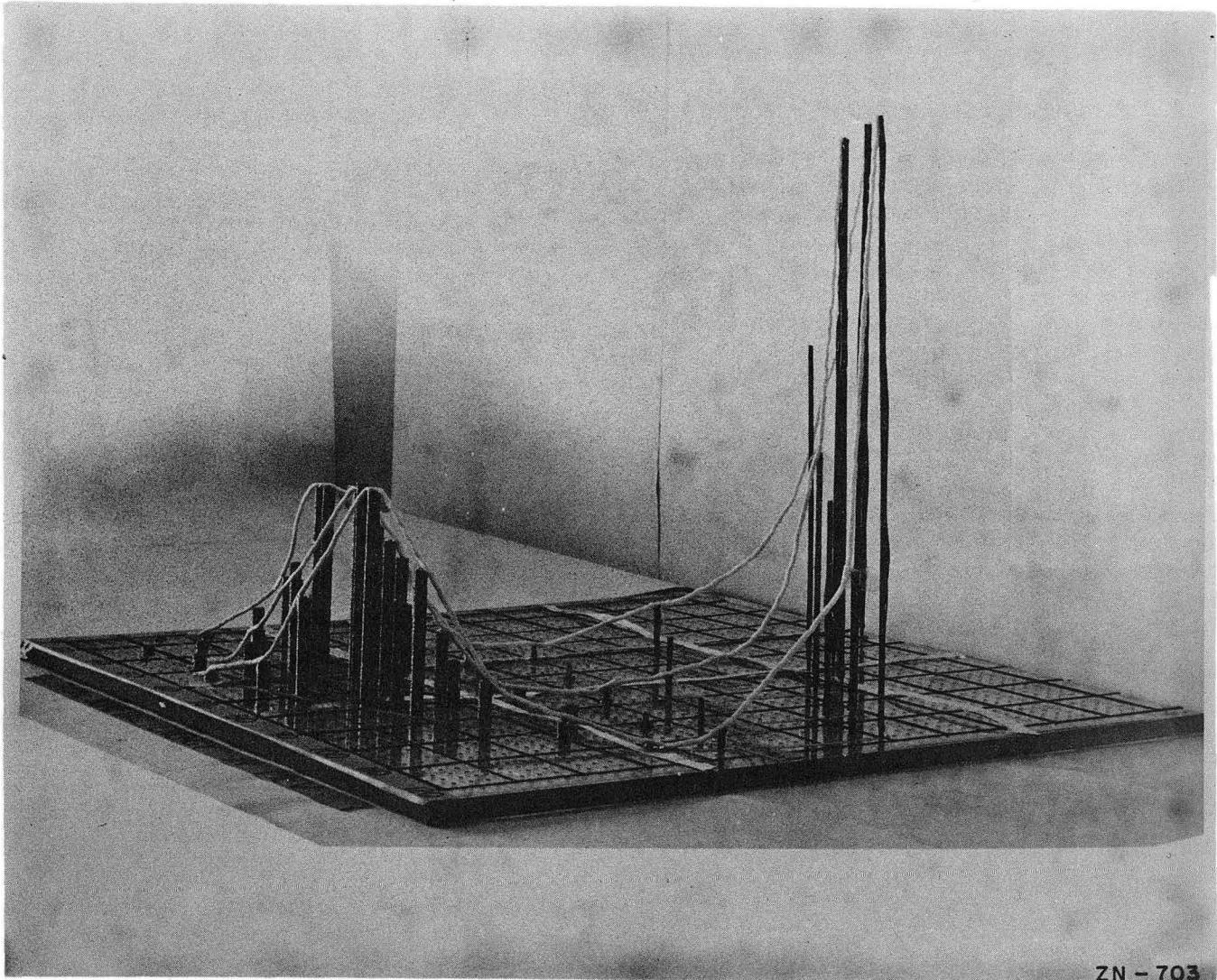
Two vertical lines are drawn on Fig. 11 to indicate the two values of minimum pion energy that were set by absorbers. These absorbers were chosen in the following way: The absorber that sets the minimum pion energy at 80 Mev separates the spin-flip spikes from the free-production peaks, for photon energies from 260 Mev to the bremsstrahlung upper limit. The experiment was planned on the basis of a knowledge of the energies of the protons and pions at only the free-production peaks and the spin-flip spikes. In terms of this two-body picture, the thinner absorber was chosen to admit the free-production energy mesons contributed by the same range of photon energies as contribute to the spikes with the thicker absorber. It is obvious that because of three-body kinematics, many photon energies can produce mesons of the same energy.

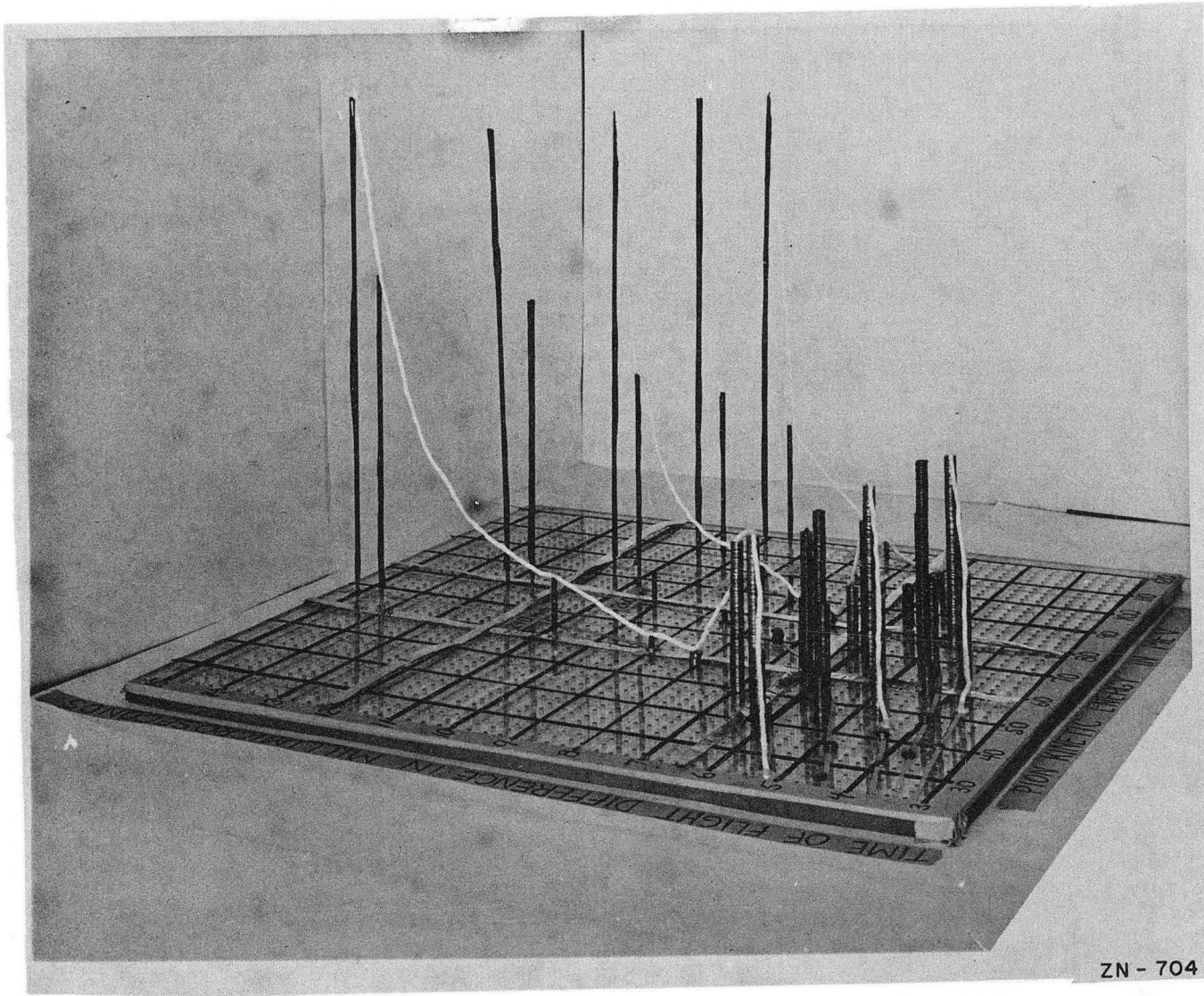
Two horizontal lines are drawn on Fig. 11 at delays of 6.38×10^{-9} sec. and 12.24×10^{-9} sec. Physically these correspond to the two lengths of delay cables used for the experiment. These delays were chosen to correspond to the low relative energy region, and with the free production region. These lines are the center of the resolution



ZN-702

Figs. 12. Various photographs of a three-dimensional model of Figure 11.





function of the equipment. As one considers delays removed from this fixed delay, the detection efficiency decreases. Nominally the pulses are clipped (i. e., differentiated by a shorted stub) to a length of 3.2×10^{-9} sec. This distance from the center of the resolution function corresponds to a detection efficiency of roughly 50 percent. At about 6×10^{-9} sec. the detection efficiency drops to zero. The delay of 12.24×10^{-9} sec. was chosen to accentuate the condition of low relative energy for the two final nucleons. The delay of 6.38×10^{-9} sec. was chosen to be near the time of flight appropriate to the free-production peaks. One can see from Figs. 11 and 12 that time of flight alone produces a fairly clean separation of the spin-flip spikes from the free-production peaks, since the detection efficiency of the coincidence system drops to zero when removed 6×10^{-9} sec. from the center of the resolution function.

One can think of the resolution function of the equipment as adding another "weight" to any point on Fig. 11. In addition, multiple-scattering nuclear absorption, the bremsstrahlung distribution, and decay in flight all "weight" any particular point of Fig. 11. The absorbers give a zero "weight" to pion energies below threshold. For any particular running condition, one delay and one absorber were used. Thus it is possible to weight the predicted spectra in four different ways, for different combinations of absorber and time-of-flight delay. This discussion gives a qualitative indication of the numerical procedure, which is described in Section VI.

E. The Measurements

The following combinations of time-of-flight delay and minimum pion energy were used in collecting data:

<u>Measurement</u>	<u>Minimum Pion Energy $T_{\pi \text{ min}}$ (Mev)</u>	<u>Delay (in 10^{-9} sec.)</u>
A	57	6.38
B	57	12.24
C	80	6.38
D	80	12.24

Measurements B and D are designed to emphasize the condition of low relative energy for the two final nucleons; hence the effect of the exclusion principle should be noticeable. In other words, a flip or no-flip spectrum should predict a noticeably different relative counting rate.

Measurements A and C are designed to emphasize the free production part of the spectra. A flip or no-flip spectrum should predict essentially the same relative counting rate. This fact is valuable in itself. The theoretically predicted ration of C to A should be in agreement with the experimentally measured numbers, independent of the spin-flip probability that we desire to measure.

When Le Levier's theory is combined with the experimental resolution of the apparatus and the geometry of the experiment, then relative counting rates for A, B, C and D can be predicted. One can then compare the ratios B/A , C/A and D/A that are theoretically predicted to those that are experimentally measured.

VI. FOLDING THE THEORETICALLY PREDICTED SPECTRA INTO THE EXPERIMENTAL RESOLUTION OF THE EQUIPMENT

A. General Discussion

Le Levier calculated the cross section per unit meson energy, for a given photon energy, with the pion at 120° and one of the protons at 20° ;

$$\frac{d\sigma(T_\pi, h\nu, \theta, \chi)}{dT_\pi d\Omega_p d\Omega_\pi} \quad \begin{array}{l} \theta = 120^\circ \\ \chi = 20^\circ \end{array}$$

In order to reduce these spectra to a counting rate that one can expect to observe in the laboratory, it is necessary to fold these theoretically predicted spectra into the bremsstrahlung spectrum and the experimental resolution of the equipment, and incorporate the particular geometry for which the experiment was performed.

Before writing down the expected counting rate in terms of the theoretically predicted spectra, it is necessary to define the following notation:

- θ = laboratory pion angle
- χ = laboratory proton angle
- N = number of counts observed
- n = number of deuterons per cm^2 in the target
- n_q = number of equivalent photons
- T_π = pion kinetic energy at production in mev
- E_1 = proton kinetic energy at production in mev
- $r(\tau')$ = resolution function of the counting equipment
(i. e., detection efficiency vs. delay)
- $\epsilon(T_\pi)$ = efficiency of detecting the pion. This includes the effect of multiple scattering, nuclear absorption, and decay in flight.
- $\frac{dn(h\nu)}{d(h\nu)}$ = number of real photons of energy $(h\nu)$ in the range $d(h\nu)$, per "equivalent" photon of integrated beam
- t_p = time of flight for the proton = $t_p(E_1, z)$
- t_π = time of flight for the pion = $t_\pi(T_\pi)$
- $\tau = t_p - t_\pi$ = difference in time of flight between the proton and the pion.
- z = target thickness in mg/cm^2 of CD_2 (total target thickness = 131)

B. Pion Time of Flight

The pion loses a negligible amount of energy in the target, air and first crystal. It loses an appreciable amount of energy only in the copper absorber next to the last crystal. Hence the time of flight is given by:

$$t_{\pi} = \frac{l_{\pi}}{c \beta_{\pi} (T_{\pi})} \quad (\text{In Millimicroseconds})$$

where: $l_{\pi} = 0.364$ meters

$$\beta_{\pi} = \frac{T_{\pi} (T_{\pi} + 2 E_{o_{\pi}})}{T_{\pi} + E_{o_{\pi}}}$$

$$E_{o_{\pi}} = 140 \text{ Mev}$$

$$c = 0.3 \text{ m } \mu \text{ sec/ meter}$$

C. Proton Time of Flight

The proton time of flight was calculated in different ways depending on the range of proton energy involved.

For proton energies greater than 20 Mev, range-energy curves were used to calculate the energy losses in the CD₂ target and in the air. Over the air path of this experiment β proton vs. proton kinetic energy is linear to less than six percent (for proton energies greater than 20 Mev); hence, it is sufficiently accurate to compute the β at the beginning and end of the air path and take the arithmetical average. Then

$$t_p = \frac{l_p}{\beta_p(E_1, z)} \quad \text{where} \quad l_p = 0.8 \text{ meter.}$$

For proton energies less than 20 Mev, the nonrelativistic expression for the kinetic energy $T_p = 1/2 Mv^2$ is in error by less than two percent. Furthermore, the percent change in β over the air path is appreciable; hence, the proton time of flight must be obtained by integration. Let T_p be the instantaneous energy of the proton. The range-energy curves for protons in air and for protons in CD₂ can be fitted empirically by power laws over the range of proton energies of interest. If E_1 is the production energy, we can easily get an expression* for $T_p(E_1, z, y)$ where z is the distance into the target measured from the face of the target nearest the proton counter and y is the distance along the air path measured from the target to the counter. Then, since $T_p(E_1, z, y) = 1/2 Mv^2$

$$t_p = \int dt = \int_{y=0}^{y=0.8 \text{ meter air}} \frac{dy}{\sqrt{\frac{2T_p(E_1, z, y)}{M}}}$$

D. The Photon Source $\frac{dn(h\nu)}{d(h\nu)}$

The full energy bremsstrahlung beam of the Berkeley synchrotron was used as the photon source. The synchrotron was operated with a "spread out" beam for which peak beam intensity occurred 1.2 milliseconds before

* See Appendix II

peak magnetic field. The theoretical bremsstrahlung spectrum has been corrected by Steinberger and Bishop^{20, 21} for this condition of operation for finite target thickness and variation of magnetic field during the expulsion period. This spectrum was used for the calculation. Figure 13 shows the relative number of photons $\frac{dn(h\nu)}{d(h\nu)}$ plotted as a function of the photon energy $h\nu$ in mev.

E. Pion Corrections

The factor $\epsilon (T_\pi)$ includes the effects of multiple scattering, nuclear absorption, and decay in flight.

The pion multiple scattering in the target, air, and first crystal is negligibly small compared to the scattering in the copper absorber between the $\pi - 1$ and $\pi - 2$ scintillators. The pion scattering in this absorber produces at most a loss of eight percent of the pions. This correction was computed as a function of pion energy for both absorbers used, using the multiple scattering with energy loss theory of Eyges.²² The rms displacement of a particle was first computed, and then its multiple scattering distribution function was integrated across the crystal width. Both these calculations were done numerically.

The nuclear absorption correction was calculated from the formula

$$\frac{n}{n_0} = e^{-\frac{(N_0 \xi) \sigma}{A}} = \text{fraction of pions remaining}$$

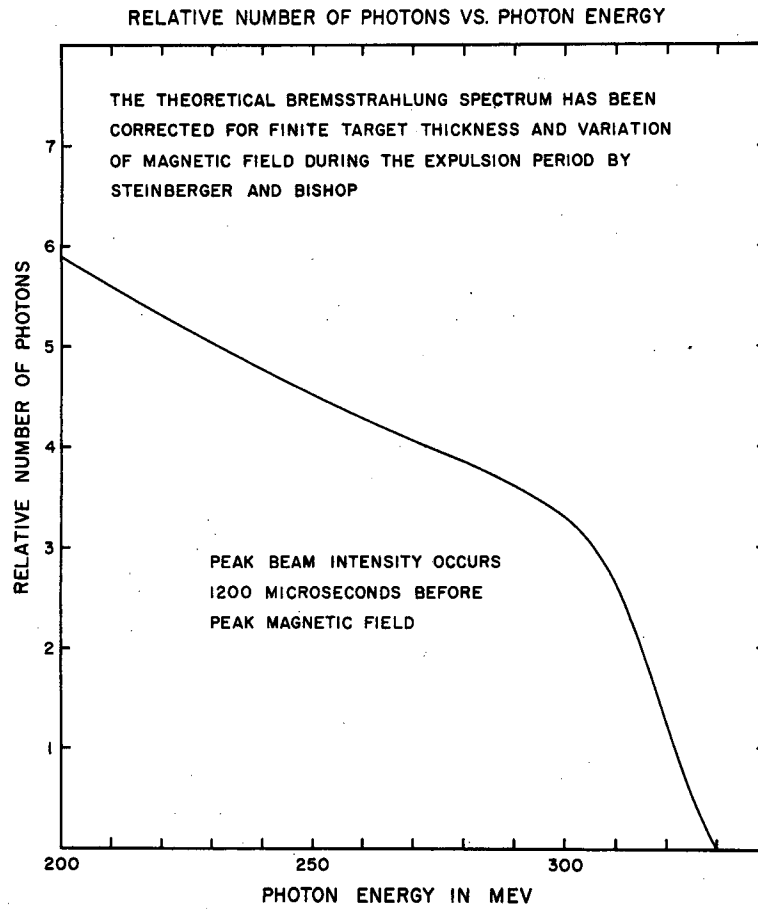
N_0 = Avogadro's number

A = molecular weight of Copper

ξ = absorber thickness in g/cm^2

$\sigma = 0.986 \times 10^{-24} = \text{cm}^2 = \text{nuclear area for copper}$

This value of σ is in good agreement with the poor geometry attenuation cross section for 85-Mev π^- mesons on copper measured by Chedester, Isaacs, Sachs and Steinberger²³, and confirmed by Stork²⁴ and others. This correction amounts to a loss of 14 percent of the pions for the thin absorber, and 23 percent of the pions for the thick absorber.



MU 5634

Fig. 13.
Relative number of photons
plotted as a function of the
photon energy.

The number of pions lost by decay in flight was calculated using the formulae:

$$\frac{N}{N_0} = e^{-\frac{t}{\tau}} = \text{fraction remaining}$$

τ was taken to be 2.54×10^{-8} seconds.

$$t = \int \frac{dt'}{\gamma} = \frac{E_0}{c} \int_0^{0.364 \text{ meter}} \frac{dx}{c p} \quad (\text{in seconds})$$

x = distance along pion path in meters

c = 3×10^8 meters/sec

p = pion momentum in Mev/c

E_0 = rest energy of negative pion = 140 Mev

The loss of pions varies from four percent to five percent, over the range of pion energies. Actually not all these pions are lost. What happens to them depends on the direction in which the muon recoils in the center-of-mass system when the pion decays. If the muon recoils backward in the center-of mass system, with respect to the original direction of the pion, then the muon is considerably reduced in energy in the laboratory relative to the original pion energy. If it recoils at right angles to the original direction of the pion, it changes the direction of the decay muon in the laboratory. If it decays in the direction of motion of the original pion, then the decay muon has an increased energy relative to the original pion. Thus muons are lost because (1) their energy is changed relative to the original pion energy, (2) the range-energy relations for pions and muons in the same material are different, and (3) some muons may be deflected through large enough angles that they do not enter the π -2 counter. Hence, the net effect is that not all the muons are lost and the five percent correction is made even smaller. This correction on the time-of-flight decay correction can be calculated in a straightforward but tedious way. It was not felt worth-while to do so since the net result of such a calculation would only decrease a five percent correction which is essentially constant and thus cancels out in taking ratios.

The various pion corrections are shown in Figures 14 and 15 as a function of pion energy. The corrections for multiple scattering, nuclear absorption, and decay in flight are shown separately. Also the total correction, which is the product of these separate factors, is shown.

F. Multiple Scattering of the Proton

It is difficult to know what type of multiple-scattering correction to apply to the proton. This difficulty stems from the fact that the reaction we are considering is a three-body reaction and thus the proton and pion which produce a coincidence are not correlated, since the angle and energy of the second proton are not known. For a two-body reaction, the multiple-scattering correction is calculable. This is possible because there is a definite correlation between the pair of angles at which the two particles are produced. The procedure in this case is described by W. J. Frank.²⁵ In the present case, however, the multiple scattering is not calculable because there is no definite angular correlation for a three-body reaction.

There are, however, some qualitative arguments that suggest that the multiple scattering may be negligible.

At the top of the free-production peak one has a two-body reaction. When we calculate production from a free neutron at rest we obtain the result $\frac{\Delta\theta}{\Delta\chi} = 2.5$ (See Fig. 1). For a case where no multiple scattering occurs, the meaning of this expression is that if the pion counter subtends δ degrees in the laboratory, then the proton counter can be $\frac{\delta}{2.5}$ degrees wide, and both counters will subtend exactly the same angle in the center-of-mass system (when both counters are centered on their two-body correlated angles).

In the present experiment both counters subtend about 7° in the laboratory. Also the worst case of proton multiple scattering gives rise to an rms multiple scattering angle of 1.8° . Hence the multiple scattering for production from a free neutron at rest would be negligible.

Similarly, the case of the spin-flip spike is essentially a two-body reaction, since the relative energy of the two final nucleons is very small for the spike. The reaction $\gamma + d \rightarrow \pi^- + 2p$ where the two protons have very low relative energy is very similar kinematically to the reaction $\gamma + d \rightarrow \pi^0 + d$. In this case $\frac{\Delta\theta}{\Delta\chi} = 2.4$ and so the multiple scattering would be negligible for the spike.

This leaves the region in between the free-production peak and the spin-flip spike. However, this region does not have as much weight as either the peak or the spike and hence is not as important.

The worst case of multiple scattering removes 30 percent of all those protons that start out in such a direction that they will hit the proton counter. When the integrations are performed, this figure is decreased. It represents an unrealistically pessimistic viewpoint because it neglects those protons that may be scattered back into the counter, and it also neglects any quasi correlation. Considering these things, the multiple-scattering correction was neglected.

G. Calculation Procedure

$$\text{The first integral } \int_0^{131} r \{ \tau(E_1, z, T_\pi) - \tau_0 \} dz$$

was performed by numerical integration. This yields a function,

$$F(E_1, T_\pi) = F(h\nu, T_\pi), \text{ since } E_1 = E_1(h\nu, T_\pi)$$

This function has two values, depending on which delay is used. The integrand of the second integral $\int_{T_{\pi \min}}^{\epsilon(T_\pi)} \frac{d\sigma(h\nu, T_\pi)}{dT_\pi} F^1(h\nu, T_\pi) dT_\pi$

was plotted as a function of T_π , and this integral was performed graphically. There are two weighting factors and two lower limits corresponding to the two absorbers that were used. This then yielded a function $G(h\nu)$. The last integral $\int \frac{dn(h\nu)}{d(h\nu)} G(h\nu) d(h\nu)$ was also performed graphically. The final result is eight numbers; the combinations of two absorbers and two delays yield four, and the use of a "flip" or "no flip" spectrum multiplies this number by two.

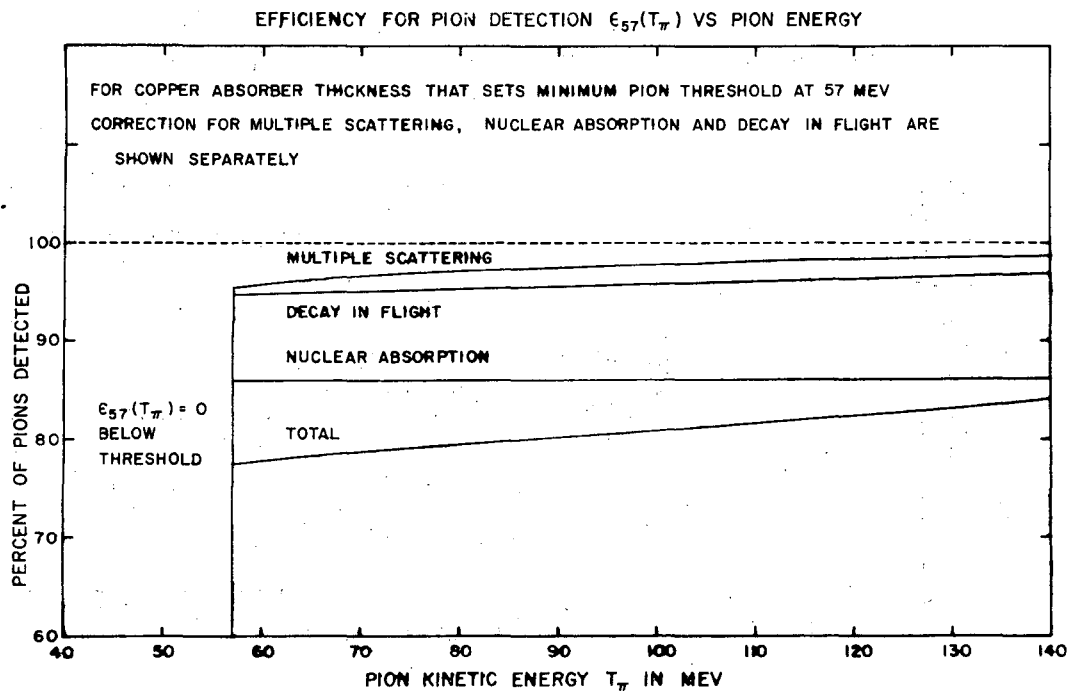
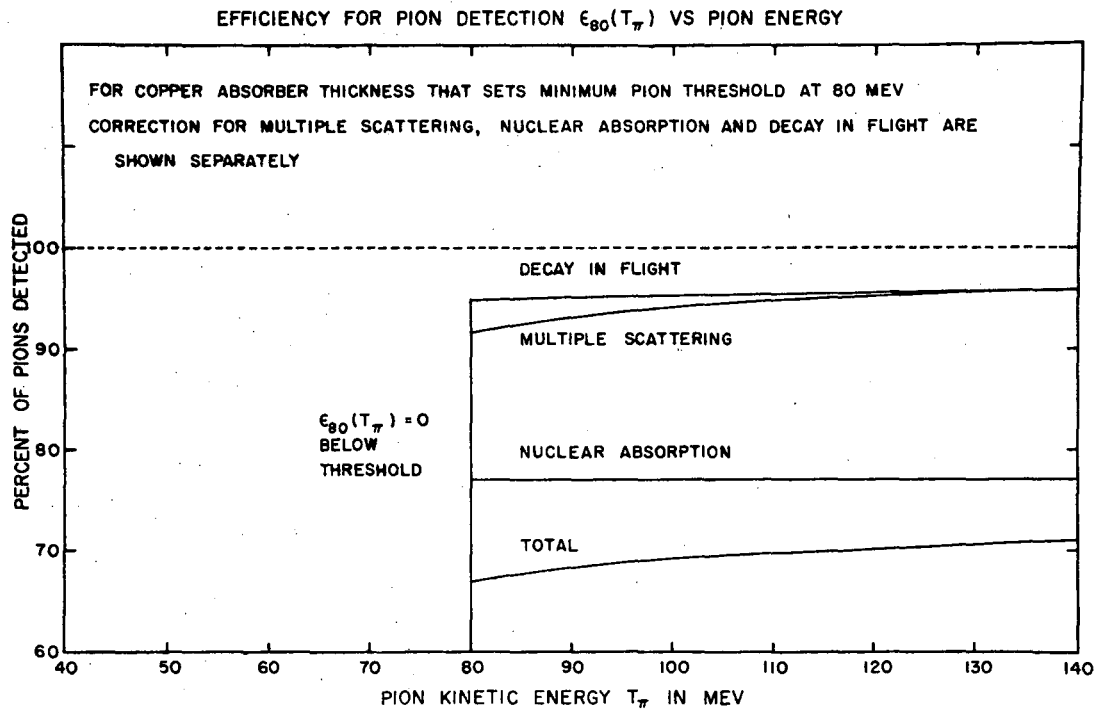


Fig. 14.

The Pion Corrections

$(T_{\pi \text{ min}} = 57 \text{ Mev})$



MU 5635

Fig. 15.
The Pion Corrections
($T_{\pi \text{ min}} = 80 \text{ Mev}$)

VII. RESULTS AND CONCLUSIONS

A. Experimental Results

The following experimental results were obtained:

Measurement	CD ₂ counts/10 nunans	CH ₂ counts/10 nunans	Difference
A	0.706 ± 0.025	0.188 ± 0.023	0.518 ± 0.034
B	0.075 ± 0.013	0.036 ± 0.011	0.039 ± 0.017
C	0.221 ± 0.015	0.089 ± 0.012	0.132 ± 0.019
D	0.021 ± 0.004	0.012 ± 0.004	0.009 ± 0.005

Standard deviations are indicated.

A "nunan" is an arbitrary amount of integrated synchrotron beam which is measured by using a precollimator ionization chamber. For the same beam level, same collimator, same operating conditions for the synchrotron, et cetera, the number of nunans is proportional to the number of photons of any particular energy. Since this is a ratio experiment, the proportionality factor is not needed, and hence the counting rate per ten nunans was taken.

About ten nunans were delivered in one minute, on the average. Thus, the counting rates given above are approximately the counting rates per minute. For measurement D we see that one difference count is obtained in about 100 minutes. This is a little more than one count in two hours, an extremely low counting rate.

One might think that cosmic radiation would be a source of background. It is not, however, because of the net delay of either six or twelve millimicroseconds inserted between the proton counter and the two pion counters. For a counter separation of one meter, one observes about 100 coincidences per hour.^{26, 27} To cause an accidental coincidence, it would be necessary for two such extensive showers to occur successively with a separation in time of either six or twelve millimicroseconds and within a time spread of about ± 3 millimicroseconds. Because of the relative infrequency with which these showers occur, it is clear that this type of event is very improbable.

Measurement A was run every few hours to insure that the equipment was operating properly and that no drifts had occurred. The period during which these data were taken extended over a period of about three weeks. The actual data-taking time was about 100 hours (61,920 nanans). Measurement A always checked within statistics. The IN54A diode resistance is temperature-sensitive, hence its bias voltage must be checked every hour or so (semi-conductors are not very temperature stable); except for this, no other adjustments were necessary.

The ratios of $\frac{B}{A}$, $\frac{C}{A}$, and $\frac{D}{A}$ calculated from the previous data are as follows:

$$\begin{aligned} \frac{B}{A} &= 0.08 \pm 0.02 \\ \frac{C}{A} &= 0.26 \pm 0.03 \\ \frac{D}{A} &= 0.017 \pm 0.007 \end{aligned}$$

where probable errors are now being quoted.

B. Relative Counting Rates Predicted from Theory

Results of calculations described in Section VI are presented below. "F" refers to a flip spectrum, and "NF" to a no-flip spectrum.

A		B		C		D	
<u>F</u>	<u>NF</u>	<u>F</u>	<u>NF</u>	<u>F</u>	<u>NF</u>	<u>F</u>	<u>NF</u>
103	90.6	16.7	0.816	14.8	12.3	5.09	0.078

If we compute the ratios from these numbers we get:

$$\begin{array}{cccccc} \frac{B}{A} & & \frac{C}{A} & & \frac{D}{A} & \\ \\ \frac{F}{A} & \frac{NF}{A} & \frac{F}{A} & \frac{NF}{A} & \frac{F}{A} & \frac{NF}{A} \\ 0.162 & 0.009 & 0.144 & 0.136 & 0.0494 & 0.0009 \end{array}$$

The disagreement of the ratio $\frac{C}{A}$ indicates that there is something basically wrong, independent of the $\frac{A}{A}$ spin-flip feature of the experiment. The trouble is that the meson theory uses a nonrelativistic approximation for the energy of the nucleons. For the free-production region, the nucleons have from 40 to 80 Mev, and in this region a nonrelativistic approximation

is not very accurate. The following table shows the effect on the free-production meson energy of using this nonrelativistic approximation for the nucleons.

Photon Energy (Mev)	Free-Production Meson Energy (Mev)	
	Using Nonrelativistic Approximation for Nu- cleon Energies	Correct Relativistic Calculation
240	42	46
260	53	57
280	62	67
300	71	76
320	79	84

This table shows that the meson energies are predicted to be about 5 Mev lower than they actually are, when this nonrelativistic approximation is made.

One would not think that a 5-Mev shift would produce such a large disagreement. It does so, however, for the following reasons: Only those pions with 80 Mev or more penetrate the thick absorber. Referring to the last table, we see that a pion whose free production energy is 80 Mev is contributed by about 310-Mev photons (correct relativistic calculation). Using the nonrelativistic calculation, we would say that such pions are contributed by 320-Mev pions. We need only refer to Fig. 13 to see that $\frac{dn(h\nu)}{d(h\nu)}$ decreases by a factor of 2.2 in going from 310 to 320 Mev. Thus, the fact that $\frac{dn(h\nu)}{d(h\nu)}$ is changing so rapidly in this region indicates that measurement C will be in error by a large amount.

For measurements B and D we are in a region where the protons have about 20 Mev, and using a nonrelativistic approximation for the proton energy is quite accurate. Measurement A will not be in error by as large an amount as C, because $\frac{dn(h\nu)}{d(h\nu)}$ is changing more slowly for a photon energy that would produce a free-production meson energy of 57 Mev.

C. An Approximate Correction for the Nucleon Nonrelativistic Approximation:

It is possible to make a rough correction to compensate for the error produced by this nonrelativistic approximation for the energy of the nucleons. In the first place, we recognize that the measurement of proton energy by the time-of-flight resolution is very broad; hence, an error of a few Mev in the proton energy will not produce a large error in the final result. However, as we have seen in the last section an error of a few Mev in meson energy produces a large error for some measurements.

Referring back to the last table, which shows the error in meson energy, we notice that the free-production energies are shifted by about 5 Mev on the average, and thus the error does not change more than about 20 percent for photon energies from 240 to 320 Mev. Thus, the free-production peaks are shifted in energy by about 5 Mev.

Figure 10 shows that if we go toward increasing meson energy the proton energy decreases, and vice versa.

This error caused by the nonrelativistic approximation will be worse for higher energy nucleons (i. e., lower energy mesons) and better for lower energy nucleons (i. e., higher energy mesons). Thus, the shift at the free-production peak is a kind of average shift over the meson spectrum. Also, the spectrum weights the free-production peak the most heavily.

Because of this kind of qualitative reasoning, it was decided that a fair correction would be to extend the limit of minimum pion energy 5 Mev lower, to compensate for the approximate 5-Mev shift produced by the nonrelativistic approximation. This was done only for the short delay, since this is where the approximation is in error. (For the long delay, the protons detected are of about 20 Mev, and hence the approximation is accurate)

The additional area produced by this integration is shown below:

	A		C	
$\frac{F}{16.2}$	$\frac{NF}{10.8}$		$\frac{F}{9.2}$	$\frac{NF}{10.5}$

If we add this correction onto the results obtained previously we get:

A		B		C		D	
<u>F</u>	<u>NF</u>	<u>F</u>	<u>NF</u>	<u>F</u>	<u>NF</u>	<u>F</u>	<u>NF</u>
119	100	16.7	0.816	25.6	22.8	5.09	0.078

Now we can recompute our ratios. The results are:

$\frac{B}{A}$		$\frac{C}{A}$		$\frac{D}{A}$	
<u>F</u>	<u>NF</u>	<u>F</u>	<u>NF</u>	<u>F</u>	<u>NF</u>
0.140	0.00816	0.215	0.228	0.0427	0.0078

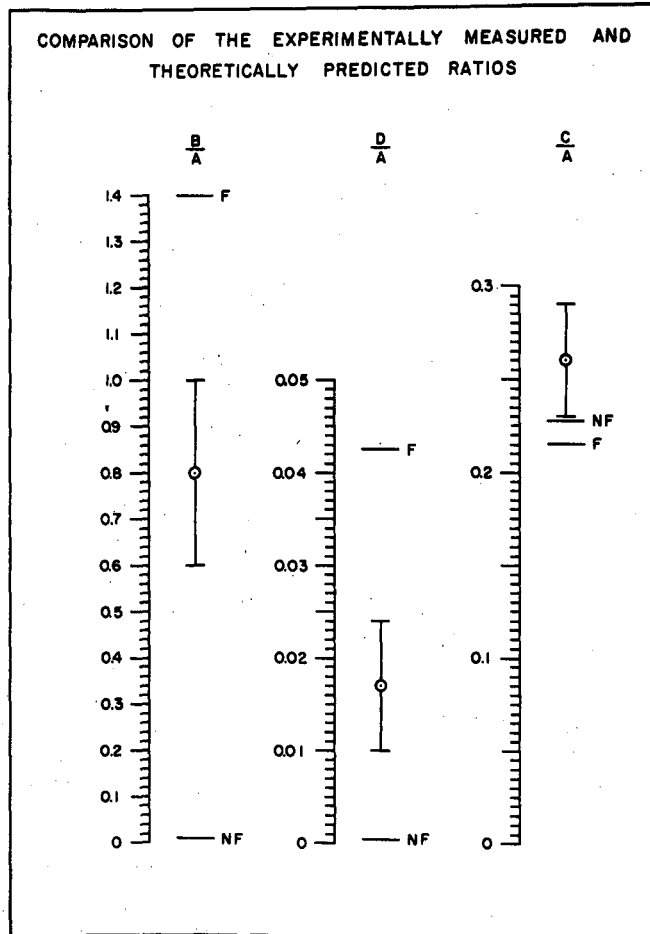
These results are certainly in much better agreement with the experimental results for the ratio $\frac{C}{A}$, which was in question. Figure 16 shows a comparison of the experimental results with the predicted results, corrected for the nonrelativistic approximation used in the theory.

D. Discussion of Results and Conclusions

Probably the first conclusion is that a correct relativistic calculation of the theory should be used to compare with experiment. The work involved in calculating these spectra is very lengthy, even when a nonrelativistic approximation is made for the energies of the two nucleons. A correct relativistic calculation would be much more lengthy. Dr. Le Levier plans to make a correct relativistic calculation, setting up the calculations on a computing machine to make possible a solution in a reasonable length of time.

So far as the rough correction for the use of a nonrelativistic expression for the kinetic energies of the nucleons in the theoretical calculations can be trusted, a few qualitative conclusions may be drawn from the experimental results.

In order to believe that theory and experiment are both valid, the ratio $\frac{C}{A}$ should be predicted accurately, since this ratio involves aspects of the theory other than the spin-flip feature. The correction that was applied tends to bring theory and experiment into closer agreement.



MU - 5778

Fig. 16.
A comparison of the experimental results with the predicted results. The predicted results are corrected for the nonrelativistic approximation for nucleon energies used in the theoretical calculations.

Hence this seems to be a step in the right direction. Furthermore, it is a step that is justified by the qualitative reasoning of the last section, and suggests that a correct relativistic calculation would give closer agreement with experiment.

Both the ratios $\frac{B}{A}$ and $\frac{D}{A}$ suggest that the interaction is neither all "flip", nor all "no flip", but rather something which is intermediate between these two extremes. The predictions of $\frac{B}{A}$ and $\frac{D}{A}$ seem to be consistent with each other, which is reassuring.

ACKNOWLEDGMENTS

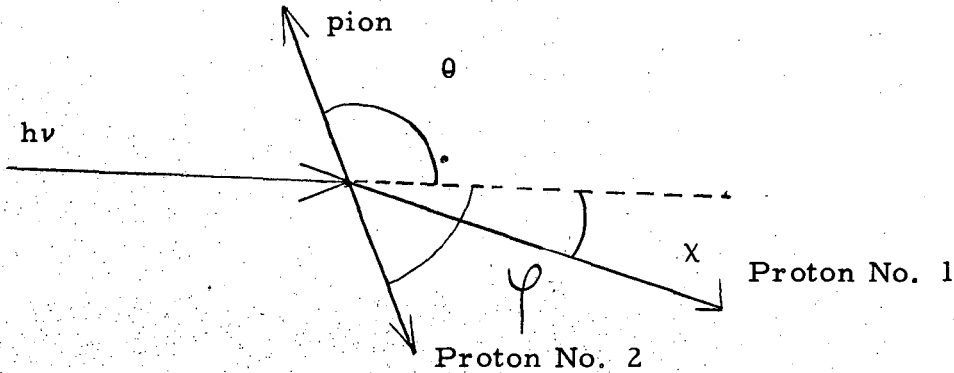
It is a pleasure to acknowledge the aid and assistance throughout of my colleagues Dr. Richard Madey and Dr. Wilson J. Frank. I wish to express my appreciation for the helpful advice and guidance of Dr. Burton J. Moyer, my graduate research advisor. I am particularly indebted to Dr. Robert E. Le Levier for many helpful discussions about the theoretical aspects of this problem.

The calculations required extensive use of the computing department's facilities, and sincere thanks are due to the whole computing staff, most of whom have worked on these calculations at one time or another. In particular, Mr. Donn Parker and Mr. Roy Morrison have spent a great deal of time on this problem and I am indeed grateful for their careful and accurate work.

Mr. Paul Nikonenko has done the major part of the engineering work for the electronic equipment used for this experiment, and it has performed reliably.

The synchrotron crew under the direction of Mr. George McFarland operated the machine efficiently and cooperated in the performance of the experiment.

Appendix I. Energy and Momentum Conservation Equations
Applied to the Reaction $\gamma + d \rightarrow \pi^- + p + p$



- Let:
- T_1 = kinetic energy of proton No. 1
 - T_2 = kinetic energy of proton No. 2
 - T_π = kinetic energy of the pion
 - T_D = kinetic energy of the center of mass of the two nucleons
 - \vec{P}_1 = (momentum of proton No. 1) $\times c$
 - \vec{P}_2 = (momentum of proton No. 2) $\times c$
 - \vec{P}_π = (momentum of pion) $\times c$
 - P_D = (momentum of the center of mass of the two nucleons) $\times c$
 - T_D = kinetic energy of the center of mass of the two nucleons
 - ϵ_f = final relative kinetic energy of the two nucleons
 - ϵ_B = binding energy of the deuteron
 - E_{O_π} = rest mass of the pion
 - E_O = rest energy of the proton

All the above quantities have the dimensions of energy. It is convenient to take the energy in units of Mev. The quantity c is, of course, the velocity of light in a vacuum.

The conservation equations applied to this reaction are:

$$\begin{aligned} \text{Energy Conservation: } h\nu &= E_{O_\pi} + T_\pi + T_1 + T_2 + \epsilon_B \\ &= E_{O_\pi} + T_\pi + T_D + \epsilon_f + \epsilon_B \end{aligned}$$

$$\begin{aligned} \text{Momentum Conservation:} \\ \vec{h\nu} &= \vec{P}_\pi + \vec{P}_1 + \vec{P}_2 \\ &= \vec{P}_\pi + \vec{P}_D \end{aligned}$$

These equations are relativistically correct if we use the correct relativistic relation between momentum and kinetic energy.

Le Levier solved the conservation equations using a non-relativistic approximation for the kinetic energies of the two nucleons, i. e. :

$$\begin{aligned} T_1 &= \frac{P_1^2}{2E_0} \\ T_2 &= \frac{P_2^2}{2E_0} \end{aligned}$$

$$\text{Hence: } T_D = \frac{P_D^2}{4M} = \frac{(\vec{P}_1 + \vec{P}_2)^2}{4M}$$

Le Levier has put these equations into a concise form for calculational purposes by making the following substitutions:

$$\begin{aligned} \vec{x} &= \frac{\vec{P}_1}{h\nu} & \vec{y} &= \frac{\vec{P}_2}{h\nu} & \vec{z} &= \frac{\vec{P}_\pi}{h\nu} \\ \eta &= \frac{h\nu}{E_0} & \xi &= \frac{E_{O_\pi}}{h\nu} & \epsilon &= \frac{\epsilon_B}{h\nu} \end{aligned}$$

Then we have the kinematical relations:

$$T_1 = \frac{h\nu}{2} \eta x^2 \quad T_2 = \frac{h\nu}{2} \eta y^2$$

$$W_\pi = \left(T_\pi + E_{O_\pi} \right) = \gamma \left(E_{O_\pi} \right) \quad z = \xi \sqrt{\gamma^2 - 1}$$

$$\epsilon_f = h\nu - W_\pi - T_D - \epsilon_B$$

Now if we divide the momentum-and energy-conservation equations by $h\nu$ we get them into the dimensionless form:

$$\text{energy: } 1 = \gamma \xi + \frac{1}{2} \eta x^2 + \frac{1}{2} \eta y^2 + \epsilon$$

$$= \gamma \xi + \frac{T_D}{h\nu} + \frac{\epsilon_f}{h\nu} + \epsilon$$

$$\text{momentum: } \vec{1} = \vec{x} + \vec{y} + \vec{z}$$

If we solve the last equation for \vec{y} , square it, substitute in the energy equation, and collect terms, we get an equation of the form:

$$x^2 - Bx + C = 0 \text{-----} (1)$$

$$\text{Where: } B = -\left[\xi \sqrt{\gamma^2 - 1} \cos(\theta + \chi) - \cos \chi \right]$$

$$C = \left[\frac{1}{2} + \frac{1}{2} \xi^2 (\gamma^2 - 1) - \xi \sqrt{\gamma^2 - 1} \cos \theta + \frac{1}{\eta} (\gamma \xi - 1 + \epsilon) \right]$$

Now, if we constrain the pion to be at 120° and one of the protons to be at 20° (i.e., at their free-production angles) by observing with counter telescopes at only those angles, then clearly:

$$B = B(\gamma)$$

$$C = C(\gamma)$$

Thus, for every value of pion energy we select, equation (1) yields two solutions for the proton energy at 20° . Only one of these solutions is observed experimentally, since the second solution corresponds to a proton at 20° whose energy is too low to detect.

Having solved for x , one can then solve for all the other quantities by using the kinematical relations. The results of this procedure are illustrated in Fig. 10.

APPENDIX II.

Proton Energy at Counter in Terms of Production Energy

The range-energy curve for protons in CD_2 can be presented by

$$R = AT_p^B$$

where: $A = 1.910$

$B = 1.815$

T_p = proton energy in Mev

R = range in mg/cm^2 of CD_2

for proton energies from 8 to 30 Mev with several percent accuracy.

Also, the range-energy curve for protons in air can be represented by:

$$R = ET_p^D$$

where: R = range in meters of air NTP

T_p = proton energy in Mev

$E = 0.01878$

$D = 1.787$

for protons from 12 to 50 Mev with several percent accuracy.

Now if:

y = distance along the flight path in meters

T_p = instantaneous energy of the proton in Mev

E_1 = production energy of the proton in Mev

z = point of production in the target measured from target face
nearest proton counter in mg/cm^2 CD_2 . Total target
thickness = $131 mg/cm^2$.

t_p = flight time of proton in seconds

$c = 3 \times 10^8$ meters/sec

$Mc^2 = 938$ Mev

Using the fact that

$$T_p = \frac{1}{2} Mv^2$$

$$v = \frac{dy}{dt}$$

$$t_p = \int dt$$

we can express $T_p = T_p(E_1, z, y)$ using the empirical range-energy relations:

$$T_p = \left[\left(E_1^B - \frac{z}{A} \right)^{\frac{D}{B}} - \frac{y}{E} \right] \frac{1}{D}$$

$y = 0.8 \text{ meter}$

Hence; $t_p = \int_{y=0}^{\frac{1}{c} \sqrt{\frac{MC^2}{2}}} \frac{dy}{\sqrt{T_p(E_1, y, z)}}$

or:

$$t_p = \frac{1}{c} \sqrt{\frac{MC^2}{2}} \int_{y=0}^{y=0.8 \text{ meter}} \left[\left(E_1^B - \frac{z}{A} \right)^{\frac{D}{B}} - \frac{y}{E} \right]^{-\frac{1}{2D}} dy$$

$$t_p(E_1, z) = \frac{1}{c} \sqrt{\frac{MC^2}{2}} \left(\frac{2ED}{2D-1} \right) \left[\left(E_1^B - \frac{z}{A} \right)^{\frac{D}{B}} \right]^{\frac{2D-1}{2D}} - \left[\left(E_1^B - \frac{z}{A} \right)^{\frac{D}{B}} - \frac{0.8}{E} \right]^{\frac{2D-1}{2D}}$$

REFERENCES

1. J. Keck and R. Littauer, "Production of Photomesons from Deuterium," Phys. Rev. 86, 602A (1952).
2. J. Keck and K. Littauer, "Production of Photomesons in Deuterium," Phys. Rev. 88, 139L (1952).
3. R. Littauer and D. Walker, "Charged Photomesons from Various Nuclei," Phys. Rev. 86, 838 (1952).
4. J. A. Thie, "Photomesons from the Deuteron," Phys. Rev. 88, 420L (1952).
5. R. Madey, K. C. Bandtel and W. J. Frank, "The Photoproduction of Negative Mesons from Deuterium," Phys. Rev. 85, 771A (1952).
6. R. Madey, "The Photoproduction of Negative Pions from Deuterium," UCRL-1634, Ph.D. Thesis, unpublished, University of California, January 9, 1952.
7. H. Feshbach and M. Lax, "The Production of Mesons by Photons and Electrons," Phys. Rev. 76, 134 (1949).
8. M. Lax and H. Feshbach, "Production of Mesons by Photons on Nuclei," Phys. Rev. 81, 189 (1951).
9. G. F. Chew and H. W. Lewis, "A Phenomenological Treatment of Photomeson Production from Deuterons," Phys. Rev. 84, 779 (1951).
10. M. Lax and H. Feshbach, "Photoproduction of Mesons in Deuterium," Phys. Rev. 88, 509 (1952).
11. Y. Saito, Y. Watanabe and Y. Yamaguchi, "Meson Production by γ Rays from Deuterium," Prog. Theoret. Phys. 7, 103 (1952).
12. S. Machida and T. Tamura, "Photomeson Production from Deuteron," Prog. Theoret. Phys. 6, 572 (1951).
13. R. E. Le Levier, "Photoproduction of Negative Pions from Deuterium," Phys. Rev. 85, 771A (1952). Also private communication.
14. G. Morpurgo, "Fotoproduzione di mesoni nel Deuterio," Nuovo cimento, Vol. VIII, No. 8, 552 (1951). See also UCRL Translation 140, April 1952.
15. N. Jarmie, "The Production of Mesons by Photons at 0° ." UCRL-2159, Ph.D. Thesis, unpublished, University of California, March 1953.
16. R. S. White, "The Production of Charged Photomesons from Deuterium and Hydrogen," Phys. Rev. 88, 836 (1952).
17. I. L. Lebow, B. T. Feld, D. H. Frisch, and L. S. Osborne, "Photomeson Production from Deuterium," Phys. Rev. 85, 681 (1952).
18. R. M. Littauer and D. Walker, "Production of Photomesons," Phys. Rev. 82, 746 (1951).

19. G. Chew, "The Inelastic Scattering of High Energy Neutrons by Deuterons According to the Impulse Approximation," *Phys. Rev.* 80, 196 (1950).
20. J. Steinberger and A. S. Bishop, "The Production of Positive Mesons by Photons," *Phys. Rev.* 86, 171 (1952).
21. J. Steinberger, private communication.
22. L. Eyges, "Multiple Scattering with Energy Loss," *Phys. Rev.* 74, 1535 (1948).
23. C. Chedester, P. Isaacs, A. Sachs and J. Steinberger, "Total Cross Sections of π^- Mesons on Protons and Several Other Nuclei," *Phys. Rev.* 82, 958 (1951).
24. D. Stork, private communication.
25. W. J. Frank, "The Angular Distribution and Yield of the Process $p + d \rightarrow t + \pi^+$," UCRL-2292. (Ph.D. Thesis, Unpublished). University of California. May 18, 1953.
26. Morton A. Levine, "Measurement of the Lateral Distribution of Extensive Air Showers," *Phys. Rev.* 88, 154A (1952).
27. G. Moliere in Chapter Three of "Cosmic Radiation," by W. Heisenberg.